



HAL
open science

Antimalarial Inhibitors Targeting Epigenetics or Mitochondria in Plasmodium falciparum: Recent Survey upon Synthesis and Biological Evaluation of Potential Drugs against Malaria

Christina L Koumpoura, Anne Robert, Constantinos M Athanassopoulos,
Michel Baltas

► To cite this version:

Christina L Koumpoura, Anne Robert, Constantinos M Athanassopoulos, Michel Baltas. Antimalarial Inhibitors Targeting Epigenetics or Mitochondria in Plasmodium falciparum: Recent Survey upon Synthesis and Biological Evaluation of Potential Drugs against Malaria. *Molecules*, 2021, 26 (18), pp.5711. 10.3390/molecules26185711 . hal-03366266

HAL Id: hal-03366266

<https://hal.science/hal-03366266v1>

Submitted on 5 Oct 2021

HAL is a multi-disciplinary open access archive for the deposit and dissemination of scientific research documents, whether they are published or not. The documents may come from teaching and research institutions in France or abroad, or from public or private research centers.

L'archive ouverte pluridisciplinaire **HAL**, est destinée au dépôt et à la diffusion de documents scientifiques de niveau recherche, publiés ou non, émanant des établissements d'enseignement et de recherche français ou étrangers, des laboratoires publics ou privés.



Distributed under a Creative Commons Attribution 4.0 International License

Review

Antimalarial Inhibitors Targeting Epigenetics or Mitochondria in *Plasmodium falciparum*: Recent Survey upon Synthesis and Biological Evaluation of Potential Drugs against Malaria

Christina L. Koumpoura ¹, Anne Robert ¹, Constantinos M. Athanassopoulos ² and Michel Baltas ^{1,*}

¹ CNRS, LCC (Laboratoire de Chimie de Coordination), Université de Toulouse, UPS, INPT, Inserm ERL 1289, 205 Route de Narbonne, BP 44099, CEDEX 4, F-31077 Toulouse, France; christina.koumpoura@lcc-toulouse.fr (C.L.K.); anne.robert@lcc-toulouse.fr (A.R.)

² Synthetic Organic Chemistry Laboratory, Department of Chemistry, University of Patras, GR-26504 Patras, Greece; kath@chemistry.upatras.gr

* Correspondence: michel.baltas@lcc-toulouse.fr



Citation: Koumpoura, C.L.; Robert, A.; Athanassopoulos, C.M.; Baltas, M. Antimalarial Inhibitors Targeting Epigenetics or Mitochondria in *Plasmodium falciparum*: Recent Survey upon Synthesis and Biological Evaluation of Potential Drugs against Malaria. *Molecules* **2021**, *26*, 5711. <https://doi.org/10.3390/molecules26185711>

Academic Editors:

Diego Muñoz-Torrero,

Simona Rapposelli,

Michael Gütschow, Maria João Matos,

Maria Emilia de Sousa and

Luciano Saso

Received: 7 August 2021

Accepted: 16 September 2021

Published: 21 September 2021

Publisher's Note: MDPI stays neutral with regard to jurisdictional claims in published maps and institutional affiliations.



Copyright: © 2021 by the authors. Licensee MDPI, Basel, Switzerland. This article is an open access article distributed under the terms and conditions of the Creative Commons Attribution (CC BY) license (<https://creativecommons.org/licenses/by/4.0/>).

Abstract: Despite many efforts, malaria remains among the most problematic infectious diseases worldwide, mainly due to the development of drug resistance by *P. falciparum*. Over the past decade, new essential pathways have been emerged to fight against malaria. Among them, epigenetic processes and mitochondrial metabolism appear to be important targets. This review will focus on recent evolutions concerning worldwide efforts to conceive, synthesize and evaluate new drug candidates interfering selectively and efficiently with these two targets and pathways. The focus will be on compounds/scaffolds that possess biological/pharmacophoric properties on DNA methyltransferases and HDAC's for epigenetics, and on cytochrome bc1 and dihydroorotate dehydrogenase for mitochondrion.

Keywords: malaria; epigenetic; mitochondria; synthesis; activities; drug candidates

1. Introduction

Malaria is the most prevalent mosquito-transmitted infectious disease worldwide affecting humans. It is caused by *Plasmodium* parasites, namely five species infecting humans (*P. falciparum*, *P. vivax*, *P. ovale*, *P. malariae*, *P. knowlesi*). Among them, the most threatening for human health is *P. falciparum*. In 2019, the number of malaria cases is reported to have exceeded 220 million causing 400,000 deaths, mostly in Africa [1,2]. While an efficacious vaccine is reported to be underway [3], chemical therapies remain the main methods to reduce the burden of malaria. Nowadays, due to malaria resistance to existing drugs, the only WHO-recommended first-line treatments are five artemisinin-based combination therapies (ACTs) [4]. Unfortunately, it is noteworthy that the emerging resistance of *P. falciparum* to the most effective drug, artemisinin, and in general to ACTs, has now spread in areas of southern Asia, making the prospects for malaria treatment concerning [5,6]. Therefore, the development of novel antimalarial drugs targeting essential and alternative biological pathways is an urgent need to control malaria worldwide and to reduce the risk of cross-resistance.

In the last fifteen years, two essential pathways have been emerged as important targets to fight against malaria, which are the epigenetic [7] and mitochondrial [8,9] processes. The purpose of this review is to evaluate the last eight years (2014–2021) on the worldwide efforts to conceive, synthesize and evaluate new drug candidates interfering selectively and efficiently with epigenetic and mitochondrial biological targets and pathways.

2. Epigenetics: A New Antimalarial Biological Target

Epigenetics is considered a new molecular target in *P. falciparum*. It regulates the general pattern of gene expression through mechanisms interfering with specialized nu-

clear architecture, histone modifications and chromatin-associated noncoding RNAs [10]. Epigenetic changes confer phenotypic plasticity to the parasite, thus, facilitating its proliferation. Histone modifications [11] and, more recently, the identification of DNA cytosine methylation [12] and hydroxymethylation [13] in *P. falciparum* makes the whole epigenetic system a potential drug target in the search of new antimalarials.

As far as the epigenetic targets are concerned, we will first present the findings (conception, synthesis, evaluation) referring to DNA methylation and then to the histone deacetylase inhibitors (HDACs). A strong biological update has recently been made that rests the focus on these inhibitors [14–17].

2.1. DNMT Antimalarial Inhibitors

The genome of *P. falciparum* contains only one bioinformatically-predicted gene with a DNA methyltransferase-2 (DNMT2) enzyme family domain (PF3D7_0727300). In 2013, Ponts et al. [12] first reported that there is a low level of DNA cytosine methylation activity in the recombinant *Pf*DNMT2 domain. Since then, many groups interested in inhibiting human DNMTs were able to obtain compounds potentially active in inhibiting *Pf*DNMTs. In that respect, recently, quinazoline-based human DNMT3a inhibitors, conceived as analogs of the known molecule BIX-01294, showed antimalarial activity on unknown targets (Figure 1) [18].

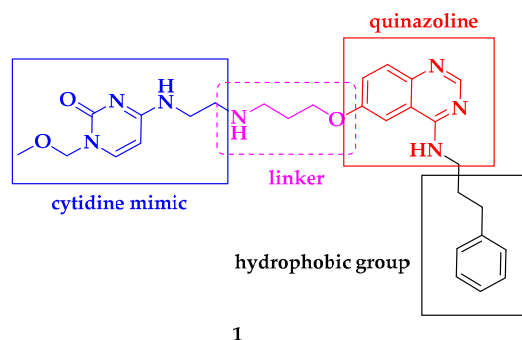


Figure 1. Quinazoline-based human DNMTa inhibitors.

In 2017, Arimondo et al. [19] identified quinoline–quinazoline bi-substrate inhibitors of human DNMT3a and DNMT1. By elaborating a strong chemical library, they obtained three compounds exhibiting the inhibition of all *P. falciparum* asexual blood stages and reducing DNA methylation in *Plasmodium* (Figure 2) [20].

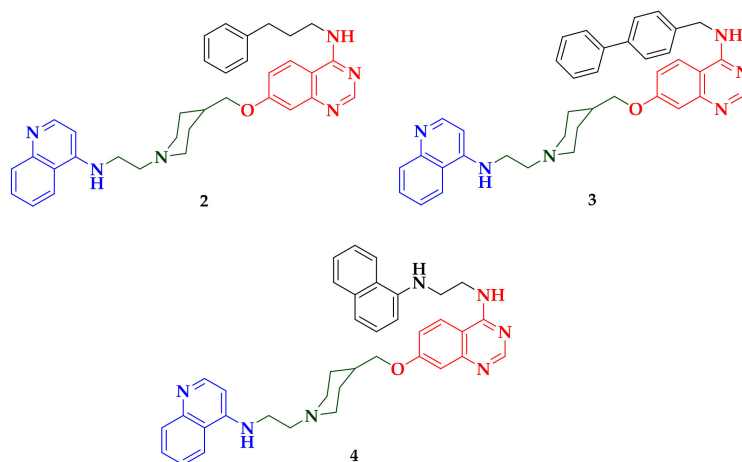
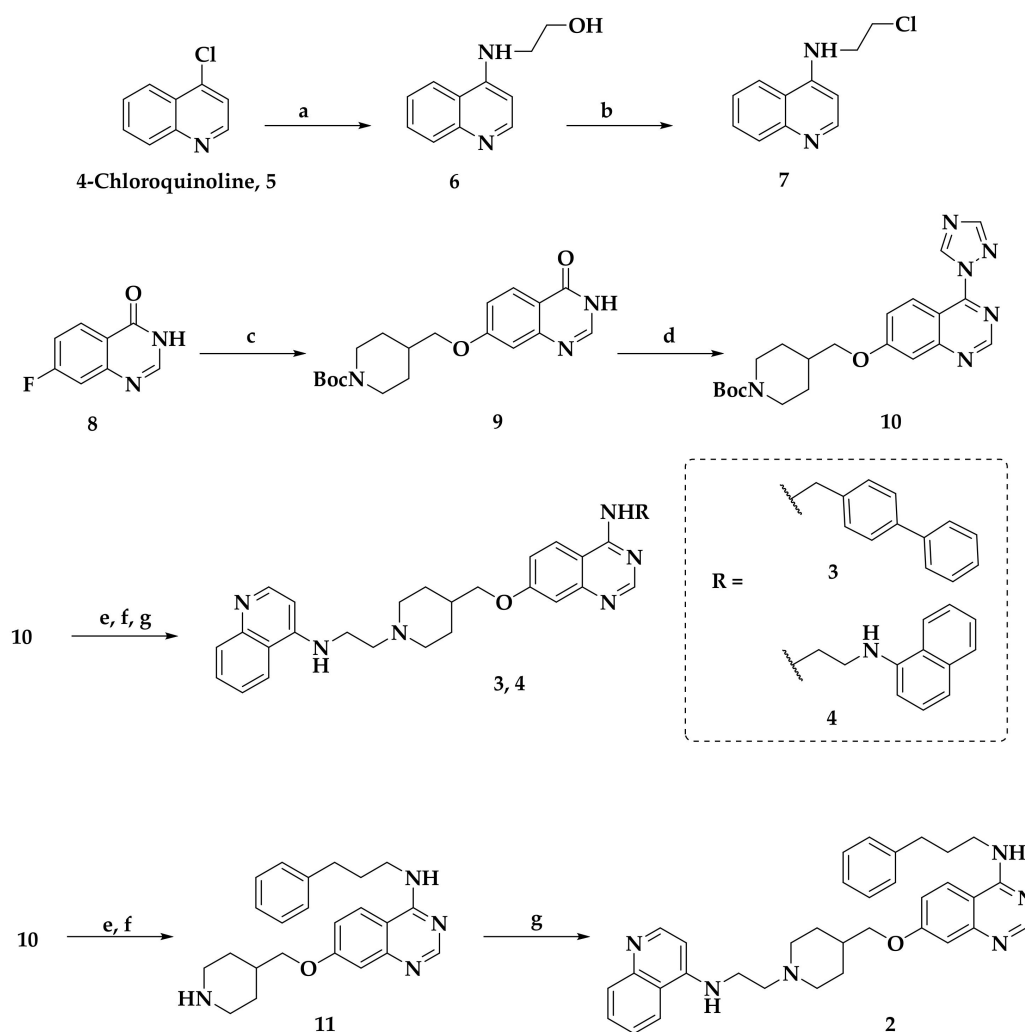


Figure 2. Bi-substrate inhibitors of human DNMT3a and DNMT1.

The main characteristics concerning these three compounds are that (i) all of them possess a quinoline scaffold at one end and an amino-quinazoline scaffold at the other end and (ii) a very important and specific linker with a cyclic piperidine methanol moiety connects these two scaffolds together.

The key elements in the synthetic route adopted by the authors are developed and shown below (Scheme 1) [19,20]. Quinoline **7** was first obtained in a two-step procedure and 91% yield from 4-chloroquinoline **5** after a reaction with ethanolamine, followed by thionyl chloride treatment. Starting from 7-fluoro-quinazoline derivative **8**, the authors first decided to introduce the *N*-Boc methanol-piperidine moiety. Afterward, chlorination of the pyrazolinone group, following a two-step procedure used in pyrimidine chemistry [21], resulted in the formation of the 4-triazolyl-quinazoline intermediate **10** in 66% total yield. Compound **10** was allowed to react with phenylpropyl amine, which upon *N*-Boc-deprotection with TFA, afforded compound **11**. Coupling of the piperidine frame with the quinoline derivative **7** led to the target compound **2** in an overall yield of 61% from **10**. Compound **10** was also used for the synthesis of target compounds **3** and **4**. The sequence of reactions is the same as before affording compound **3** in 29% yield and **4** in 45% starting from compound **10**.



Scheme 1. Synthetic pathway leading to compounds **2**, **3** and **4**. Reagents and conditions: (a) ethanolamine, 125 °C, 4 h, quant.; (b) SOCl₂, DMF (cat.), flash boiling, 91%; (c) *N*-Boc-4-methanollpiperidine, NaH, DMF, 110 °C, 3 h, 67%; (d) POCl₃, 1,2,4-triazole, Et₃N, MeCN, 18 h, rt, 66% two-steps; (e) amine, Et₃N, DMF, rt or 65 °C, 2–6 h; (f) TFA, rt, 1 h; (g) **7**, K₂CO₃, KI, DMF, 65 °C, 12 h; Yields **2** (61%); **3** (29%); **4** (45%).

The authors determined that the IC_{50} on *P. falciparum* NF54 strain for compounds 2, 3 and 4 were 71 ± 23 , 513 ± 63 and 60 ± 14 nM, respectively (Table 1). This study showed, through *in vitro* tests, that the two most potent molecules of the library (2 and 4) significantly inhibit DNA's methylation. In addition, they were found to be equally active against four Cambodian multidrug-resistant strains (5150, 6591, 5248, 6320) and able to overcome cross-resistance [20]. They were also studied *in vivo* to examine the parasite clearing. The authors proved that the water-soluble compound 2 can completely reduce the infection on a murine model.

Table 1. Proliferation inhibition of asynchronous asexual cultures of *P. falciparum* NF54 and HepG2 Cells ^a.

Compound	<i>P. falciparum</i> (nM)	HepG2 Cells (nM)
2	71 ± 23	1400 ± 200
3	513 ± 63	ND
4	60 ± 14	2500 ± 500
Dihydroartemisin (DHA)	5 ± 1	ND

^a Mean $IC_{50} \pm SD$ (standard deviation) of at least two independent experiments run in triplicate. ND: not determined.

Thus, compound 2 exhibited a positive correlation between *in vitro* and *in vivo* anti-malarial activity and the reduction of DNA methylation. Sentence to be changed as: This series of compounds can be considered as the first one incorporating a potential drug candidate for inhibition of the DNMTs of *P. falciparum*.

2.2. Histone Deacetylase (HDAC) Inhibition

Histone deacetylases (HDACs), as important epigenetic modulators [22–24], have been extensively involved in the therapeutic investigation of many human diseases, especially cancer. Today, there are four anticancer HDAC inhibitors (vorinostat, panobinostat, belinostat, and romidepsin) that have been clinically approved by the US FDA [25–29], while the promising drug candidate quisinostat is currently in phase II of clinical trials [30] against tumors (Figure 3).

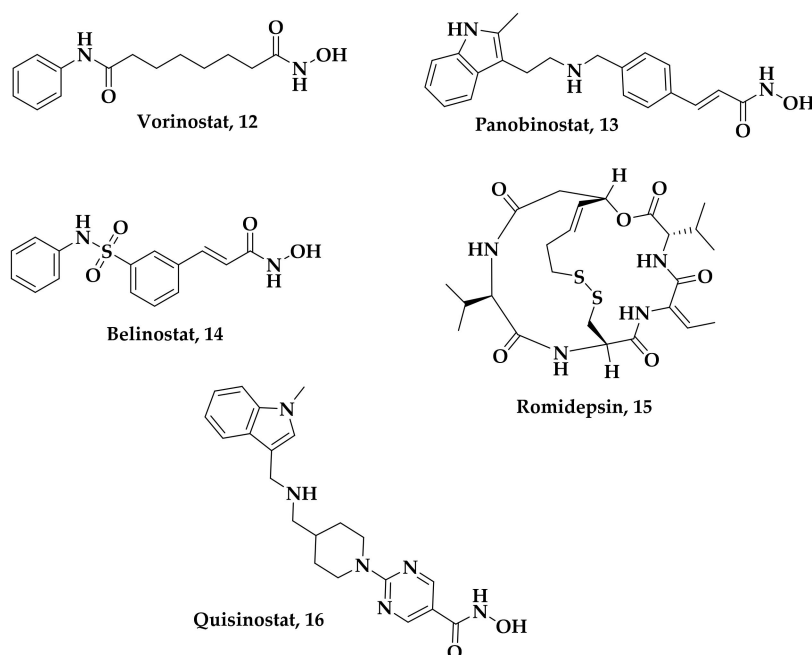


Figure 3. US FDA-approved anticancer HDAC inhibitors.

Concerning the *Plasmodium* parasite, five *P. falciparum* HDACs have been identified (*Pf*HDACs) until recently [31–33]: (i) class I-type *Pf*HDAC1, which has homology to mammalian class I isoforms, (ii) class II-type *Pf*HDAC2 and *Pf*HDAC3, presenting Zn^{2+} cations in their active site and are also similar to class II mammalian HDACs, and (iii) class III-type *Pf*Sir2A and *Pf*Sir2B which use NAD^+ as a cofactor and are the silent information regulator 2 (SIR2) proteins. In general, *Pf*HDACs regulate the acetylation level of both malarial histone and nonhistone proteins and play a critical role in the survival and reproduction of parasites. Since the pioneering discovery of apicidin (**17**) (Figure 4) in 1996 [34], several groups have launched research programs focusing on the therapeutic potency of *Pf*HDAC inhibitors. However, no *Pf*HDAC inhibitor has successfully reached clinical treatment or study despite more than two decades of research. This could be a result of the difficulty of the *in vivo* tests and consequently on pharmacokinetic studies. As a result, only erythrocytic therapeutic aspects have been tested on some compounds.

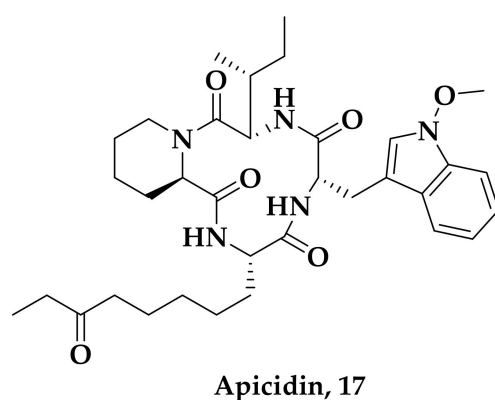


Figure 4. Structure of apicidin.

Although the four clinically approved antitumoral HDAC inhibitors (**12**, **13**, **14** and **15**) are reported to show antimalarial activity in the nanomolar range, their low selectivity prevents them from going through further clinical studies [35]. Nevertheless, their efficiency to kill malaria parasites renders *Pf*HDACs important targets for antimalarial drug discovery and development.

In 2016, Ontoria et al. reported [36] a new series of *P. falciparum* growth inhibitors. Inspired by two compounds, vorinostat (**12**), which effectively kills the parasites *in vitro*, and compound **18** that presents efficacy against malaria in animal models, the authors firstly developed a novel series of heterocyclic compounds elaborated as inhibitors of human class-I HDACs. This new series of molecules is well represented by compound **19** (Figure 5). This library is based on: (i) a central imidazole frame that displays the pharmacophore elements common to many inhibitors of HDAC enzymes, (ii) a zinc-binding group (ZBG) potentially interacting with the catalytic metal ion of the HDAC enzyme, attached by an alkyl linker and (iii) two surface contact groups (the aryl and the amide group) potentially interacting at the entrance of the substrate-binding channel. Taking into consideration many compounds of this structural class, the authors oriented their efforts in developing new selective inhibitors of *Pf*HDAC1. After several efforts and trying to overcome the detrimental effect on oral absorption caused by the basic amido functionality, they managed to introduce the electroneutral thiazole amide fragment.

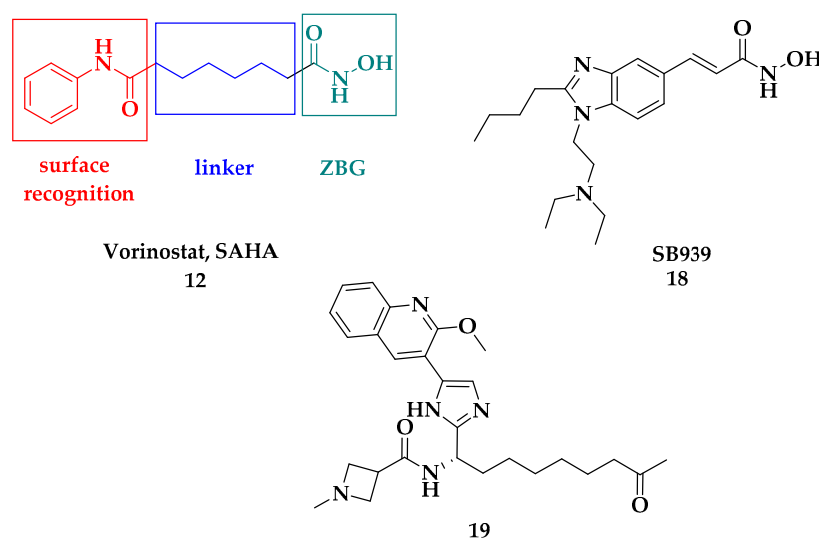
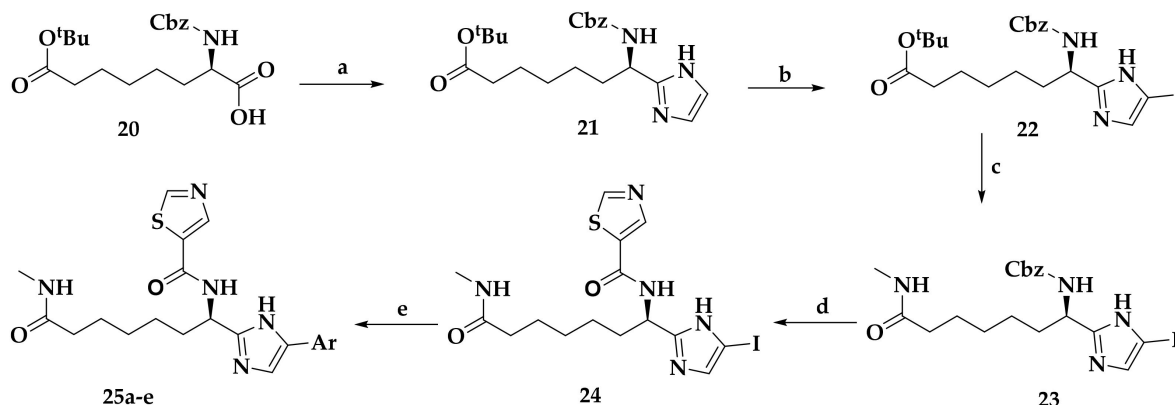


Figure 5. Structures of known human HDAC inhibitors.

The strategy of the synthesis of the above-mentioned compounds is illustrated in Scheme 2. Starting from the known amino acid **20**, [37] an imidazole ring was installed in three synthetic steps [38]. The halogenation/dehalogenation protocol was then applied for the obtention of the desired mono-iodinated compound **22** (total yield 88% starting from **20**). Ester deprotection of **22**, followed by coupling with methylamine, afforded the synthetically versatile intermediate **23** in 96% yield. Removal of the Cbz- protecting group and reaction with thiazole-2-carboxylic acid led to compound **24** (total yield 91% starting from **20**). The Suzuki cross-coupling reaction between **24** and boronic acids (or esters), when using PdCl₂ as a pre-catalyst, furnished compounds **25a–e**, with yields varying between 46% and 95% for this final step.



Scheme 2. Synthetic pathway leading to compounds **25a–e**. Reagents and conditions: (a) (i) MeNHOMe.HCl, HBTU, DIPEA, DMF, rt; (ii) LiAlH₄, THF, −20 °C; (iii) glyoxal, NH₃, MeOH, rt, 93% (3 steps); (b) (i) NIS, CH₃CN, −10 °C; (ii) Na₂SO₃, Bu₄NHSO₄, dioxane/water, 160 °C, μw, 30 min., 84% (2 steps) (c) (i) TFA, DCM, rt; (ii) MeNH₂, HBTU, DMF, rt, 96% (2 steps); (d) (i) HBr in CH₃COOH, DCM, 0 °C to rt; (ii) thiazole-2-carboxylic acid, EDC.HCl, HOBT, DIPEA, DMF, rt, 90% (2 steps); (e) ArB(OH)₂, PdCl₂ (dppf), K₂CO₃, DME/water, 110 °C. Yields **25a** (95%); **25b** (46%); **25c** (55%); **25d** (62%); **25e** synthesized by alternative analogous procedures (2 steps quantitative).

The authors evaluated the activities of their compounds against *Pf* growth (EC₅₀ values obtained) and against HeLa class I HDAC and *h*HDAC1 (IC₅₀'s determined) (Table 2). Their results highlighted, that in respect to inhibition of human class I HDAC and HeLa cells, both potency and selectivity on *Plasmodium* growth were strongly influenced by

acid-focused chemical library. The first approach concerns the diverse-oriented four components Ugi reaction. However, the second methodology applied provides access to many more compounds and it was conducted by two submonomer pathways. This approach circumvents the problem of the isocyanides involved in the Ugi reaction which are toxic and have limited commercial availability because of chemical space. This second approach is presented in Scheme 3.

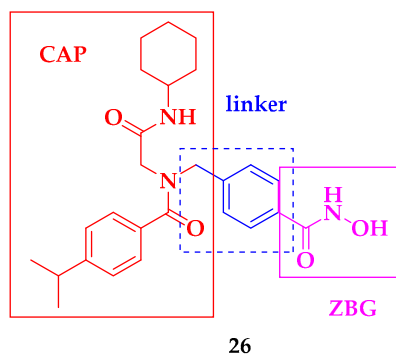
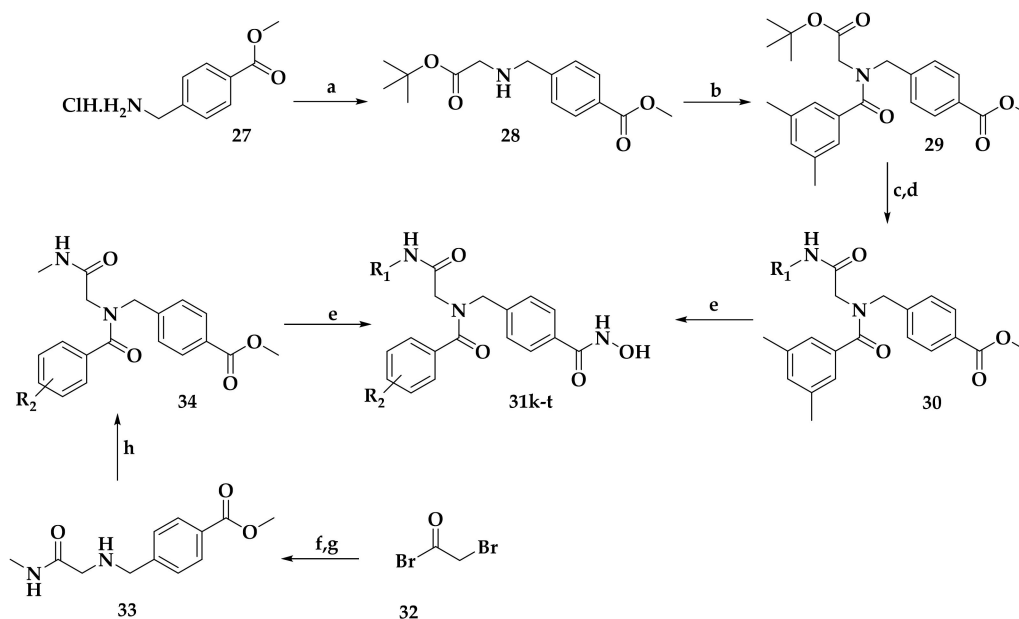


Figure 6. Structure of compound 26.



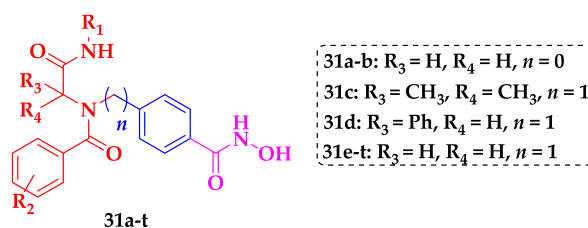
Scheme 3. Synthetic pathways leading to peptoid-based hydroxamic acids **31k–t**. Reagents and conditions: (a) ^tButyl bromoacetate, Et₃N, THF, rt, 46%; (b) 3,5-dimethylbenzoyl chloride, Et₃N, DCM, rt, 99%; (c) (i) TFA/DCM (1:1), rt, 99%; (d) R₁-NH₂, EDC, DMAP, Et₃N, DCM, rt, 80%; (e) H₂NOH (aq.), NaOH, DCM/MeOH (1:3), rt, yields 24–91%; (f) Methylamine hydrochloride, K₂CO₃, DCM, 46%; (g) methyl 4-(aminoethyl)benzoate hydrochloride, Et₃N, THF, rt, 50%; (h) R₂-Ph-COCl, Et₃N, DCM, rt, yields 46–88%.

In the first submonomer pathway, methyl(4-aminomethyl) benzoate hydrochloride (**27**) was reacted with *tert*-butyl bromoacetate and subsequently acylated with 3,5-dimethyl benzoyl chloride leading to *tert*-butyl ester **29** in 73% yield (2 steps). After deprotection of the *tert*-butyl group and EDC-mediated amide coupling reactions and aqueous hydroxylamine hydrochloride using hydroxylamine and sodium hydroxide, the final hydroxamic acid derivatives **31k–r**, were obtained in medium to good yields. Hydroxamic acids **31s–t**, were prepared *via* the second submonomer pathway, starting with a reaction of bromoacetyl bromide **32** with methylamine hydrochloride, followed by a reaction of substitution with

4-amino methyl benzoate hydrochloride affording the secondary amine **34** in medium yields. Acylation of the amine **34** with two different benzoyl chlorides followed by hydroxylaminolysis finally led to the target compounds, while the range of yields of this final step varies between 46% and 88%.

All synthesized compounds were screened and assessed for their antiplasmodial activities and human cell (HepG2) cytotoxicities. Most of them displayed IC_{50} values ranging from 0.0052 to 0.25 μM against asexual blood-stage *P. falciparum* parasites (3D7 line) and selectivity indexes from 170 to 1483 over mammalian cells. The authors suggest that the greatest impact on SAR and STR results is especially due to the carboxylic region (R_1). They also suggest that certain structural modifications on the isocyanide and carbonyl region improve cytotoxicity. In addition, some compounds showed submicromolar activity against *P. berghei* exo-erythrocytic forms, with the compound **31h** emerging as the dual-stage antiplasmodial HDACi (IC_{50} (Pf3D7) = 0.0052 μM , IC_{50} (PbEEF) = 0.016 μM) one with specific parasite activity. The authors also point out that several compounds (**31c**, **31e**, **31s**, **31t**) developed in the series showed interesting antiplasmodial activities, IC_{50} (Pf3D7) = 0.0052–0.12 μM , and good selectivity indexes, SI = 417–889, thus, representing a valuable starting point for the development of novel drug candidates (Table 3).

Table 3. *In vitro* results against asexual intraerythrocytic stage *P. falciparum*.



Compound	R_1	R_2	Pf3D7 IC_{50} (μM)
31c	c-Hex	4-(CH_3) ₂ N	0.095 \pm 0.015
31e	^t Bu	2- CH_3	0.11 \pm 0.080
31h	Bn	4- ⁱ Pr	0.0052 \pm 0.0036
31s	CH_3	3,5- CH_3	0.054 \pm 0.0029
31t	CH_3	2- CH_3	0.071 \pm 0.015
SAHA (12)	-	-	0.17 \pm 0.035
Chloroquine	-	-	0.0068 \pm 0.0023

Ruoxi Li et al. reported this year [45] their results of a new series of PfHDAC1 inhibitors with dual-stage antimalarial potency and improved safety which was based on structural modifications of quisinostat. Quisinostat (**16**) showed potent antimalarial *in vitro* activity [46] and inhibited both wild-type and drug-resistant *P. falciparum* strains with IC_{50} values 5–7 nM. Based on these findings, the authors elaborated a focused library of 31 novel hydroxamic acid derivatives and evaluated their efficacy as antimalarials. Similar to other HDAC inhibitors, the authors conceived their structures considering the three important components of quisinostat: an hydroxamic acid that chelates the Zn^{2+} cofactor in the catalytic pocket (ZBG), an *N*-methylindole fragment (CAP region) entering in favorable interactions with the amino acid residues at the entrance of the catalytic pocket and the linker between these two entities that is a pyrimidinyl 4-aminomethyl piperidine fragment (Figure 7). The authors focused on the modification of the linker, while the critical scaffolds of hydroxamic acid and indole were mainly preserved. Concerning the linker, the authors oriented their efforts towards the introduction of a rigid spirocyclic moiety [47], in contrast to the most widely applied flexible aliphatic diamine linkers existing in HDAC inhibitors' strategy.

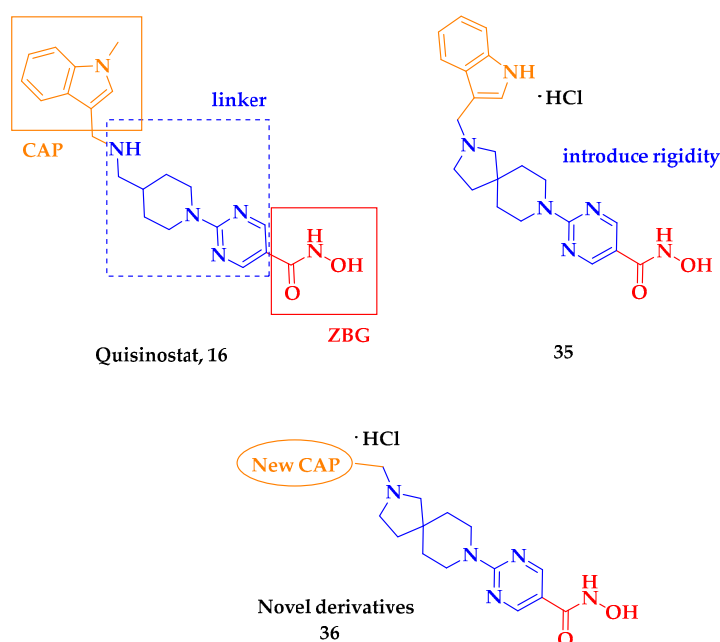
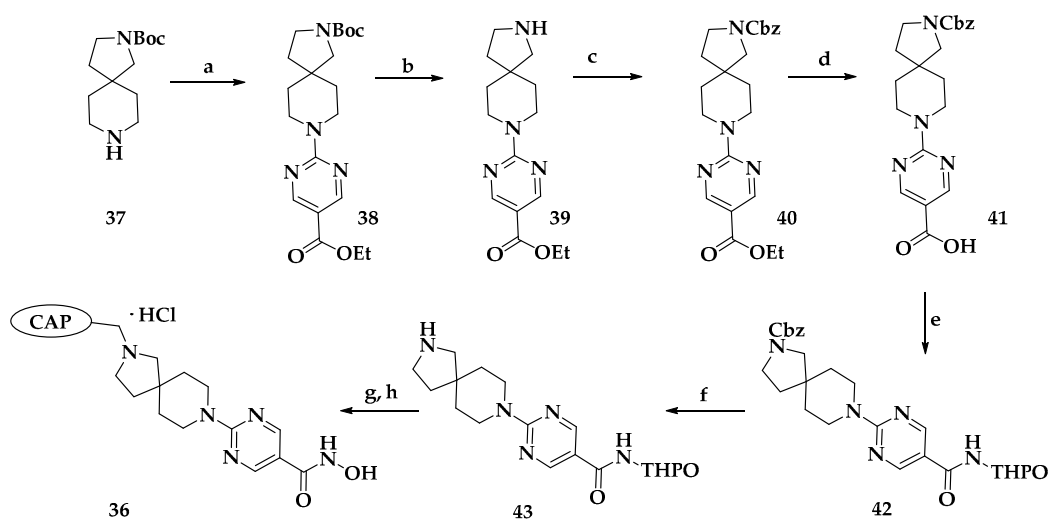


Figure 7. Some new spirocyclic hydroxamic acid derivatives.

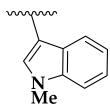
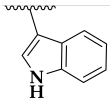
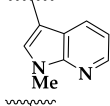
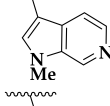
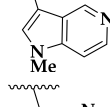
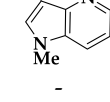
Scheme 4 presents the synthesis of spirocyclic derivatives **36** via a different method from that already reported for quisinostat [48]. *Tert*-butyl-2,8-diaza spiro-(4,5)-decane-2-carboxylate (**37**) was coupled with ethyl 2-chloropyrimidine carboxylate under alkaline conditions to afford ester **38** in 86% yield. A two-step modification of the protective group (Cbz vs. Boc) by acid elimination of Boc and installation of the benzyloxy carbonyl group led to compound **40** in 94% yield. Further hydrolysis of the ethyl ester providing the appropriate carboxylic acid was followed by conversion into **42** via condensation with *O*-(tetrahydro-2H-pyran-2-yl) hydroxylamine in excellent yields. Hydrogenolysis of the Cbz group afforded the intermediate **43** possessing a free secondary amine. This function was then coupled under reductive amination conditions with a variety of aldehydes leading to the final compounds **36** with yields varying between 20% and 30% for this final step.



Scheme 4. Synthesis of novel derivatives **36**. Reagents and conditions: (a) ethyl-2-chloropyrimidine-5-carboxylate; *i*-Pr₂NEt, DCM, rt, 86%; (b) HCl/1,4-dioxane (4M), DCM, rt, quantitative; (c) PhCH₂OC(O)Cl, *i*-Pr₂NEt, DCM, rt, 87%; (d) K₂CO₃, MeOH, H₂O, 65 °C; (e) THPONH₂, EDCI, HOBT, Et₃N, Me₂NCHO, rt, 82% (2 steps); (f) Et₃SiH, Pd/C, MeOH/DCM (1:1), rt; (g) R-CHO, NaBH₃(CN), MeOH rt; (h) HCl/1,4-dioxane (4 M), DCM, rt (20–30% 3 steps).

All compounds were tested and compared to **16** for antimalarial potency and cytotoxicity. Six derivatives, **36a–f**, inherit the nanoscale IC₅₀ values of **16** against drug-sensitive and chloroquine-resistant *P. falciparum* parasites while their cytotoxicity is attenuated 3–10 times, due to the central diamine spirocyclic fragment (Table 4). Compounds **36a–f**, were also evaluated against five clinical *Pf* isolates carrying various phenotypes of resistance including artemisinin-resistant parasites. As IC₅₀ values between these and wild-type parasites are similar, the authors concluded that the compounds can be good candidates against antimalarial drug resistance.

Table 4. *In vitro* results against erythrocytic stage in *P. falciparum* of compounds **36a–f** ^a.

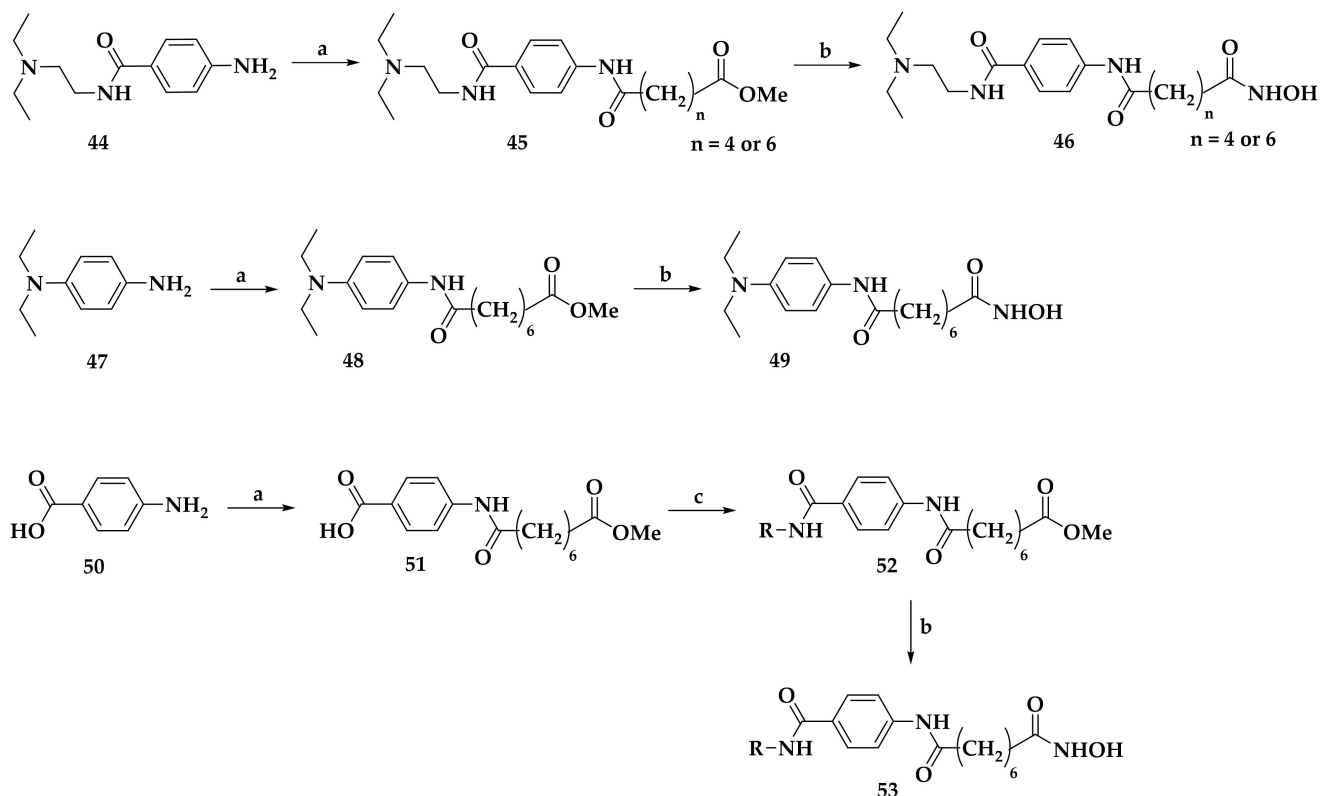
Compound	CAP	Erythrocytic IC ₅₀ (nM) ^a		SI
		3D7	Dd2	
36a		2.8 ± 0.2	2.5 ± 0.1	22
36b		3.19 ± 0.07	1.9 ± 0.1	75
36c		3.0 ± 0.2	3.4 ± 0.3	132
36d		3.0 ± 0.5	5.6 ± 0.1	180
36e		4.0 ± 0.1	4.9 ± 1.2	370
36f		3.22 ± 0.02	4.3 ± 0.3	235
DHA	-	2.7 ± 0.2	2.68 ± 0.02	ND

^a Results are the mean ± SD obtained from two independent biological repeats, DHA = dihydroartemisinin, ND = Not Determined.

The same compounds showed enhanced metabolic stability in comparison to quisinostat (**16**). However, only **36b** prevents asymptomatic liver stage infection and targets *Pf*HDAC1. In that respect, the authors consider that compound **36b** could represent a new starting point for antimalarial drug development.

In addition, very recently, Arimondo's group reported [49] a new generation of compounds targeting *h*HDAC6, but the same compounds were also found to be very active against *P. falciparum*. Their strategy was based on constructing dual inhibitors, combining the histone deacetylase inhibitor SAHA with the DNMT inhibitor procainamide [50] in a compound called Proca-SAHA [31]. The authors found this compound to be active against the *P. falciparum* asexual blood-stage (IC₅₀*Pf* = 41 nM), showing a 50-fold better selectivity index than SAHA alone. Afterward, they conducted a focused structure–activity relationship study and reported seven new compounds in which the number of methylene groups of the linker and/or the terminal amide group were modified.

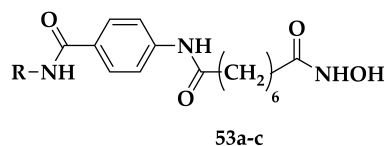
The synthetic procedure followed for the preparation of this series of compounds is presented in Scheme 5.



Scheme 5. Synthesis of hydroxamate derivatives. Reagents and conditions: (a) methyl 8-chloro-oxooctanoate or methyl 6-chloro-6-oxohexanoate, TEA, DMF, 18 h, rt, yields 70–98%; (b) NH_2OH 50%, MeOH, 18 h, rt, yields 42–88%; (c) HATU, DIPEA, DMF, appropriate amine, 4 h, rt, yields 38–72%.

Compounds **46** were synthesized by direct coupling between procainamide and the corresponding acyl chlorides of the methyl oxonate derivatives in excellent yields. The chemical modulation of compounds **46** was achieved via a three-step synthetic pathway starting either from *N,N*-diethyl-*p*-phenylene diamine or from 4-amino benzoic acid. Only compound **53c** needs a further step due to the presence of a Boc-protecting group which needs to be eliminated in the end. All the obtained compounds were evaluated against *P. falciparum*. The results indicated that the molecules possessing six methylene groups plus a secondary or tertiary amino basic group at the extremity of the chain are the most potent with IC_{50} values varying between 41 nM and 64 nM (Table 5), while all other compounds showed values between 230 nM and 500 nM. The authors identified that the lead compound **53c** is highly potent against *hHDAC6* with no cytotoxicity in human cancer cells, but most importantly, highly active against multiple *P. falciparum* isolates from Cambodia. The authors also presented *in vivo* results where the same compound delays the onset of parasitemia when injected intraperitoneally in a *P. berghei* severe malaria model. This result is better than the one observed with SAHA in a non-severe malaria murine model [41]. Finally, they concluded that a rapid, cheap, already obtained synthetic route along with a needed pharmacokinetic modulation of compound **53a** could lead to a new antimalarial therapy.

Table 5. Inhibition on the proliferation of asynchronous asexual cultures of *Plasmodium falciparum* NF54 and HDAC activity against human (*h*HDAC1, 2, 3 and 6) and parasite extracts by Proca-SAHA derivatives.

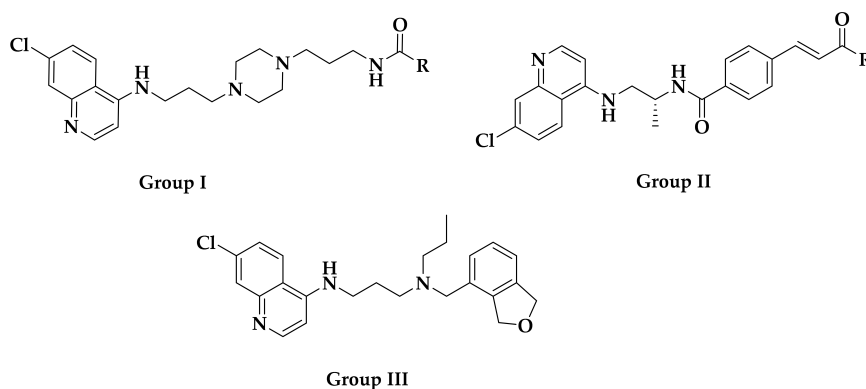


Compound	R	<i>Pf</i> Mean IC ₅₀ (nM)	<i>h</i> HDAC Extracts IC ₅₀ (μM)	<i>Pf</i> HDAC Extracts IC ₅₀ (μM)
53a		41 ± 7	0.06 ± 0.05	0.38 ± 0.07
53b		64 ± 2	0.16 ± 0.01	ND
53c		52 ± 12	0.14 ± 0.07	0.48 ± 0.07
SAHA	-	175 ± 33	0.18 ± 0.07	0.46 ± 0.11
DHA	-	3 ± 7	-	-

Finally, we will finish this first chapter on epigenetics and *Plasmodium* growth-inhibition with a detailed study reported in 2018 by Kumar et al. [51] on *in silico* identification of inhibitors against *Pf* histone deacetylase 1 (*Pf*HDAC1). In this study, the authors conducted comparative modeling studies of the *Pf*HDAC1, using Modeller v9.14 [52]. Afterward, they proceeded with molecular modeling to establish different binding modes of non-selective and selective compounds in the *Pf*HDAC1 active site. They, thus, identified four non-identical active site residues located on the surface and slightly away from the catalytic machinery. These residues affect the selectivity of the compounds by imposing different directional interactions and binding modes inside the catalytic pocket. The authors have also applied virtual screening with precise selection criteria and molecular dynamics simulation. Their work permitted them to select twenty potential inhibitors of *Pf*HDAC1: ten coming from the ChEMBL and ten from analogs compound libraries by screening the ZINC and PubChem databases. Finally, the identified compounds were categorized into seven groups based on their structural scaffolds.

Among these compounds, sixteen are known antimalarials and fourteen are reported to have activities in the nanomolar range against various drug-resistant and sensitive strains of *P. falciparum*. As a result, they could be used as potential HDAC1 inhibitors against *P. falciparum* as their evaluated cytotoxicities are at relatively high concentrations.

Groups I and III (10 compounds) possess a secondary amide group as zinc-binding moiety, thus, addressing HDAC selectivity in *P. falciparum* (Table 6). The docking score of reported ChEMBL bioactive antimalarial compounds against *Pf*HDAC1 was found to vary between −10.715 kcal/mol (ChEMBL152862) and −9.117 kcal/mol (ChEMBL211750). Their predicted binding affinities (X score) are in the range of −10.52 kcal/mol (ChEMBL3103569) to −8.11 kcal/mol (ChEMBL1197874). They all form at least one hydrogen bond and seven hydrophobic contacts with residues within the *Pf*HDAC1 active site. In that respect, the H-bond interactions forming, involve E94, D97, G147, and H176 amino acids whereas the hydrophobic ones involve residues H24, A95, H138, H139, C149, F203, L269, G298, G299, and Y301 (Table 7).

Table 6. Reported antimalarial activity of the identified potential HDAC1 inhibitors in *P. falciparum* ^a.

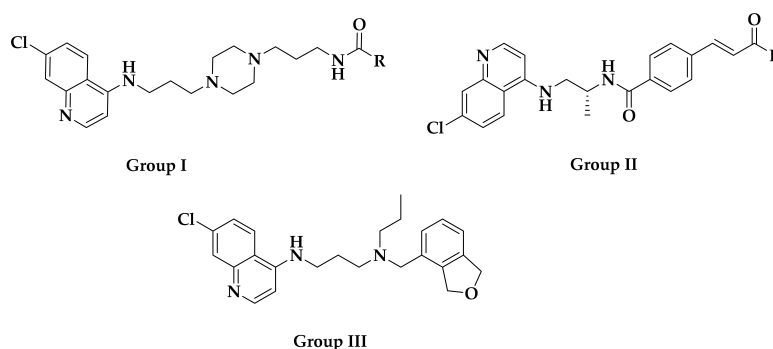
Compound ID	Group	R	Reported Activity (Target) ^a
CHEMBL152862	I		IC ₅₀ : 289.2 ± 25.8 nM (A) IC ₅₀ : 34 nM (B)
CHEMBL244454	I		IC ₅₀ : 78 nM (C) IC ₅₀ : 13 nM (D)
CHEMBL152635	I		IC ₅₀ : 159 nM (C) IC ₅₀ : 19 nM (D)
CID: 11730425	I		IC ₅₀ : 34.7 nM (A)
CHEMBL3103569	II		IC ₅₀ : 110 nM (E) IC ₅₀ : 80 nM (F)
CHEMBL211750	III	-	IC ₅₀ : 3.3 nM (E) IC ₅₀ : 1.9 nM (F)

^a **Targets:** (A) *Pf* chloroquine-resistant strain FcB1; (B) *Pf* histidine-rich protein; (C) *Pf* chloroquine- and pyrimethamine-resistant strain K1; (D) *Pf* chloroquine-sensitive strain NF54; (E) *Pf* multidrug-resistant strain W2; (F) *Pf* isolate 3D7. **In silico data:** In Table 7 are reported docking and X scores of the above-mentioned compounds.

As far as the compounds from the analogs compound library are concerned, they also present the docking score in the range of −10.315 kcal/mol (CID:11730425) to −9.671 kcal/mol (ZINC101453222) and X score in the range of −8.76 kcal/mol (CID:11122900) to −8.01 kcal/mol (CID:10916465).

Finally, comparatively to benchmark compounds (Table 5), the 20 identified by the authors' study have a lower docking score and predicted binding affinity, suggesting that they may perform as better inhibitors of *Pf*HDAC1 than the benchmark ones.

The authors consider that these findings are important for developing new prospective antimalarials, also pointing out the potential advantage of the nonidentical residues which can be exploited to design selective inhibitors against *Pf*HDAC1.

Table 7. Results on molecular docking of selected inhibitors against *Pf*HDAC1 active site and their predicted binding affinity (X score).

Compound ID	Group	R	Docking Score (kcal/mol)	Predicted Binding Affinity (X Score) (kcal/mol)
CHEMBL152862	I		-10.715	-8.52
CHEMBL244454	I		-10.529	-8.80
CHEMBL152635	I		-10.116	-8.42
CHEMBL3103569	II		-9.723	-10.52
CHEMBL211750	III	-	-9.117	-8.13
CID: 11730425	I		-10.315	-8.64
Vorinostat	-	-	-8.019	-7.74
Pracinostat	-	-	-7.336	-8.39
Panobinostat	-	-	-3.897	-7.69
Belinostat	-	-	-2.432	-8.43

3. Malaria Focused Mitochondrial Targets

We will discuss here some recent findings concerning the inhibition of two main targets of *Plasmodium* mitochondrion that are also biochemically related: cytochrome bc1 and dihydroorotate dehydrogenase (DHODH) [53,54].

Cytochrome bc1 is a multi-subunit heterodimer localized in the inner mitochondrial membrane. The subunit composition can vary depending on living organisms: 3 units for bacteria, 11 units for vertebrates, 10 units for yeast [55–58]. They all possess a catalytic domain containing three essential subunits: cytochrome c, cytochrome c1 and the Rieske iron–sulfur protein [59]. Cytochrome bc1 (bc1 for short) is the key element for the function of the mitochondrial electron transfer process briefly described as follows: ubiquinol is oxidized to ubiquinone in the oxidative Q₀ site, resulting in the release of two protons into the intermembrane space. Ubiquinone is then subsequently reduced at the reductive Q_i site back to ubiquinol by up-taking two protons from the matrix [60,61]. Into the parasite, the oxidized ubiquinone from bc1 is used by dihydroorotate dehydrogenase to generate orotate which is an essential intermediate in pyrimidine biosynthesis.

The first bc1 structure was determined in 1997 by X-ray crystallography at 3.0 Å resolution, after isolation from bovine mitochondria [57,58]. Since then, numerous well-resolved X-ray structures of bc1 from various species have been reported, such as bovine [62], chicken [63], yeast [64], and *Rhodobacter* [65], thus, providing better insight into the structure/activity and mechanism relationships inside the bc1 complex.

The dihydroorotate dehydrogenase (DHODH) enzyme catalyzes the fourth step in the *de novo* pyrimidine biosynthesis [66,67], i.e., the flavin mononucleotide-dependent oxidation of *L*-dihydroorotate to orotate. For *Plasmodium* parasites, the *de novo* pyrimidine synthesis is an essential pathway for their survival [68] as *Plasmodium* lacks any salvage pathways to generate pyrimidines. In this respect, two compounds are already reported as DHODH inhibitors. Compound DSM265 (54) is currently in phase II of clinical trials with activities against both asexual blood-stage and liver-stage parasites. Along with compound DSM421 (55), they are the most well studied and clinically relevant antimalarial DHODH inhibitors [69]. It is worth mentioning that they both bear a fluorinated triazolopyrimidine scaffold (Figure 8).

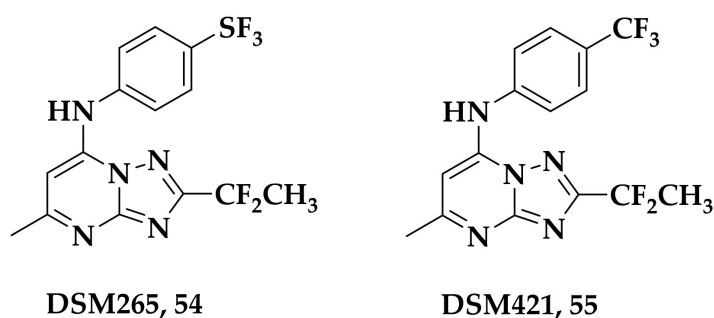


Figure 8. DHODH inhibitors in clinical trials.

3.1. Atovaquone: A *bc1* Inhibitor

Concerning the cytochrome complex, atovaquone (56) (Figure 9) is reported [70] to be the leading compound/drug against the *bc1* target. Atovaquone is approved in the market of the United States under the trade name Mepron for the treatment of *Pneumocystis carini* infection. It is also available in combination with proguanil hydrochloride under the trade name Malarone for the treatment and prevention of *P. falciparum* uncomplicated malaria [71–73]. Atovaquone is a ubiquinone analog acting as a competitive inhibitor at the Q_0 site of cytochrome *bc1* [74]. Unfortunately, the development of point mutations in the Q_0 site of cytochrome *bc1* from the parasite results in the formation of atovaquone-resistant strains, which can considerably reduce the anti-malarial efficacy of atovaquone. Nevertheless, based on atovaquone, and the primary important scaffold (commercially available) lawsone (57), many efforts have been deployed in order to find new lead compounds which could circumvent the drug resistance of the parasite.

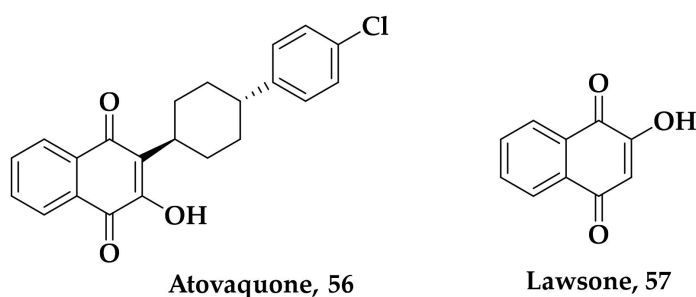
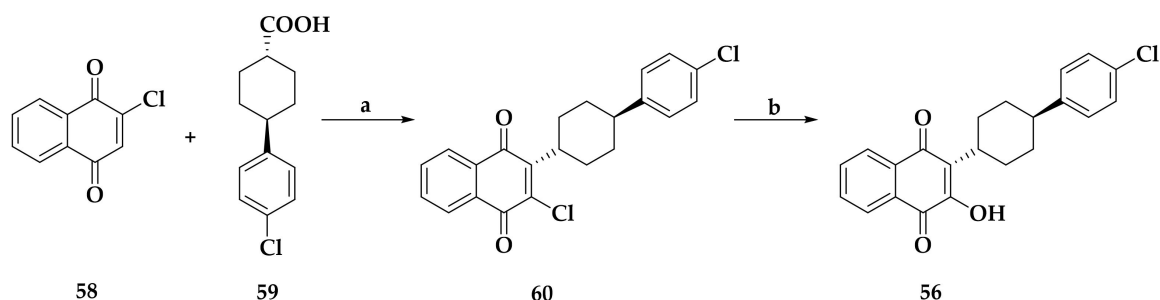


Figure 9. Structures of atovaquone and lawsone.

In this second part of the review, we focus first on the synthetic routes leading to atovaquone, then, on the recent findings concerning *bc1* and/or DHODH antimalarial inhibitors.

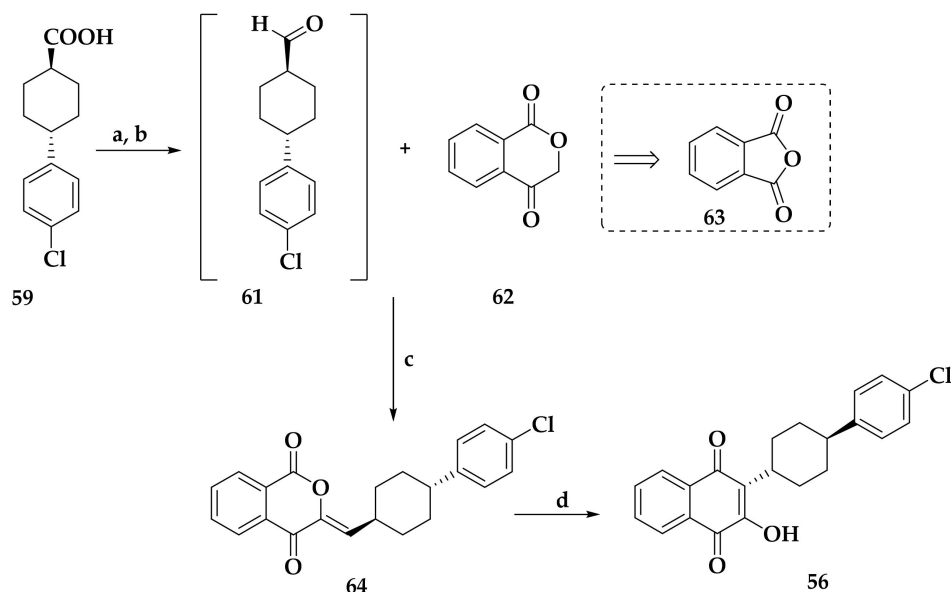
The first synthesis of atovaquone was reported by Hudson et al. [75,76]. 2-chloronaphthoquinone (58) reacts through a radical pathway with *trans*-4-chlorophenylcyclo-hexane

carboxylic acid (**59**) in the presence of AgNO_3 and ammonium persulfate (Scheme 6). Hydrolysis of the obtained chloro-atovaquone derivative **60** with methanolic KOH leads to atovaquone (**56**) in 4% overall yield. By following the same synthetic strategy, three more procedures have been reported [77–79] without better success in terms of yield and cost-efficacy.



Scheme 6. The first reported synthesis of atovaquone (**56**) by Hudson et al. Reagents and conditions: (a) AgNO_3 , $(\text{NH}_4)_2\text{S}_2\text{O}_8$, rt, 7%; (b) MeOH, KOH, rt, 58%; total yield 4%.

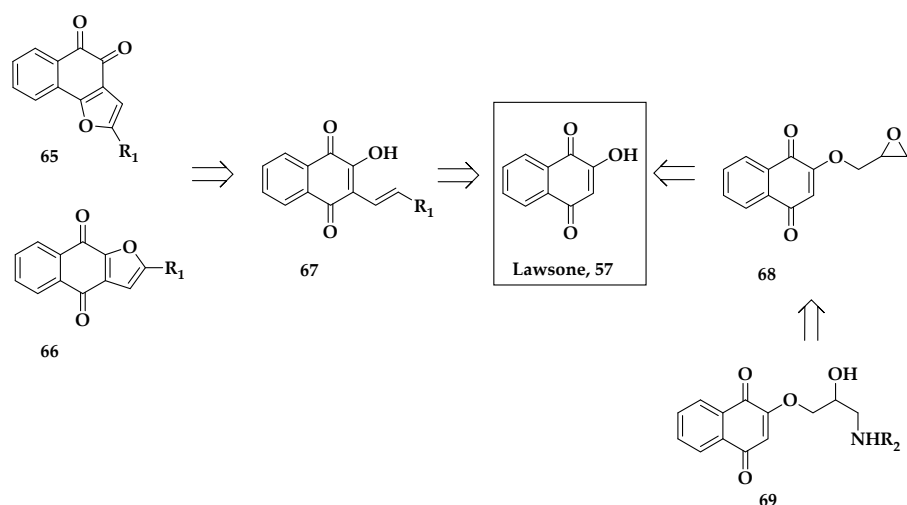
A different approach was reported by GlaxoSmithKline [80], where isochromadione **62** reacts with the *in situ* formed aldehyde **61** issued from controlled activation/hydrogenation of the trans-4-chlorophenylcyclohexane carboxylic acid **59** in the presence of isobutylamine and acetic acid. The unsaturated ketone **64** then undergoes a basic methanolic treatment leading to atovaquone with 67% yield for the two steps (Scheme 7) [81,82].



Scheme 7. GlaxoSmithKline synthesis of atovaquone (**56**). Reagents and conditions: (a) $(\text{COCl})_2$, DMF (cat.); AcOEt (b) H_2 , Pd/C, AcOEt, quinaldine; (c) CH_3COOH , Isobutylamine, 40 °C, 76%; (d) 25% NaOMe/MeOH, rt, 91%.

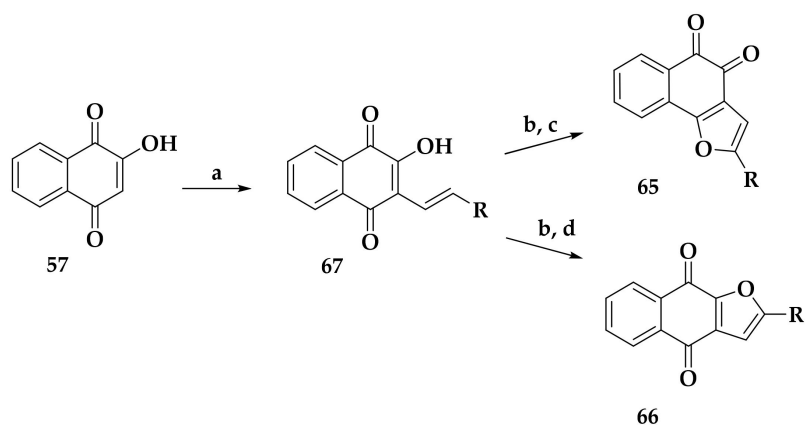
3.2. *bc1* and/or DHODH Antimalarial Inhibitors

In 2017, Borgati et al. [83] reported a series of four families of compounds issued from structural modifications of the lawsone compound and their *in vitro* antiplasmodial activities against the chloroquine-resistant *P. falciparum* W2 strain. The general retrosynthetic scheme of their work is presented below (Scheme 8).



Scheme 8. Commercially available lawsonone (57) as starting material leading to 4 different families of molecules.

Knoevenagel aldol condensation of lawsonone (57) with various aldehydes afforded the first family of dienol compounds 67 with yields varying between 32% and 91%. The second and third family of compounds are furano-naphthoquinones 65 and 66 that can be selectively obtained either by application of kinetic control (ortho-compounds 65) or thermodynamic (para-compounds 66) in yields varying between 20% and 92% (Scheme 9). The authors also synthesized a fourth series of compounds issued from a two-step reaction: etherification of the hydroxy group of lawsonone (57) by reaction with epichlorohydrin and the subsequent opening of the resulting epoxide ring with selected amines. The overall yields are quite low and oscillate between 20% and 30%.

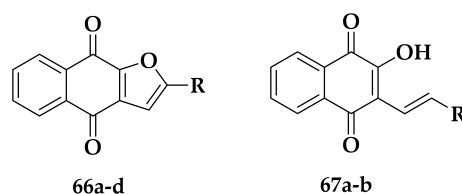


Scheme 9. Synthesis of furano-naphthoquinone analogs. Reagents and conditions: (a) CH₃COOH, R-CH₂CHO, HCl (conc.), reflux, 40 min., yields 30–90%; (b) Hg(OAc)₂, CH₃COOH, rt, 30 min.; (c) EtOH, HCl 2N, 15 min., reflux, yields 20–90% (2 steps); (d) EtOH, HCl (conc.), 15 min., reflux, yields 20–90% (2 steps).

Among all compounds tested *via* the lactate dehydrogenase method [84,85], the furano-naphthoquinone derivatives 65 and 66 were found to be the most active with more than 70% parasitemia reduction at 25 µg/mL. Cytotoxicities were also determined and showed that the para-furano-naphthoquinone derivatives have a better selectivity index than their ortho-regioisomeric analogs. Through molecular docking simulation (Auto Dock Vina software) [86], studies concerning the *Plasmodium* targets Pfcyst bc1 complex and the PfdHODH enzyme, the authors were able to demonstrate that the most favorable interactions leading to favorable binding energies (<−10 Kcal/mol) exist, especially regarding

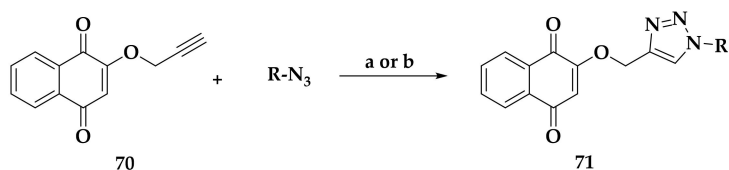
the *para*-furano-naphthoquinone derivatives **66c** and **66d** along with the most promising IC_{50} values (Table 8). Nevertheless, they point out that further experimental assays and enzymatic kinetic studies are necessary to validate that *para*-furano-naphthoquinones could work as promising hits targeting *Pf*cyt bc1 and *Pf*DHODH.

Table 8. Percentages of parasitemia reduction and *in vitro* antiplasmodial activity (IC_{50}) against *P. falciparum* (W2) for molecules **66** and **67**.



Compound	R	% Reduction at 25 μ g/mL	IC_{50} (μ M)
67a	$-\text{CH}_2\text{CH}_2\text{CH}_3$	50%	52.65 ± 3.71
67b		58%	39.55 ± 8.98
66b	$-\text{CH}_3$	75%	26.57 ± 3.25
66a	$-\text{CH}_2\text{CH}_2\text{CH}_3$	86%	11.65 ± 2.50
66c		85%	18.78 ± 0.83
66d		78%	21.80 ± 2.64
Chloroquine	-	-	0.280 ± 0.01

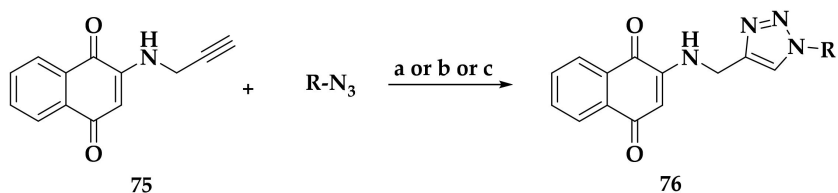
Guided by the concept of molecular hybridization, Oramas-Royo et al. reported in 2019 [87], the synthesis and antiplasmodial activities of a series of 1,2,3-triazole-naphthoquinone conjugates (Scheme 10). These compounds were synthesized through a copper(I) catalyzed Huisgen 1,3-dipolar cycloaddition [88] between O-propargylated naphthoquinone **70** and various alkyl or aryl azides with yields varying between 30% and 90%.



Scheme 10. Synthesis and structure of 1,2,3-triazole-naphthoquinone analogs **71**. Reagents and conditions: (a) $\text{CuSO}_4 \cdot 5\text{H}_2\text{O}$, sodium ascorbate, $\text{DCM}/\text{H}_2\text{O}$ (1:1), rt; (b) CuI , CH_3CN , rt; 30–98%.

The starting compound O-propargyl-naphthoquinone (**70**) was obtained by reacting 2-hydroxy-1,4-naphthoquinone and propargyl bromide in the presence of K_2CO_3 in DMF, while the aryl and alkyl azides were obtained from alkyl bromide or boronic acids and sodium azide.

The obtained 1,2,3-triazole-naphthoquinone derivatives (**71a–f**) were evaluated *in vitro* against chloroquine-sensitive F-32 Tanzania strains of *P. falciparum* and human breast cancer SkBr-3 (Table 9).



Scheme 12. Synthesis of compounds 76. Reagents and conditions: (a) Cu_2O , sodium ascorbate, acetone/ H_2O , rt; (b) $CuSO_4 \cdot 5H_2O$, sodium ascorbate, DCM/ H_2O (1:1), rt; (c) CuI , THF, rt; yields 14–86%.

The most active compounds obtained were all from the first series 71a–f. Among them, 71c and 71f proved to be the most active against *P. falciparum*, with IC_{50} values of 1.2 μM and 0.8 μM , respectively. Molecular docking on the potential target *PfDHODH* was also carried out by the authors, by using the reported X-ray crystal structure of *P. falciparum* (Protein Data Bank (PDB 1TV5) [89,90], demonstrating that compound 71c has substantial binding affinities and very favorable interactions in the active site of DHODH enzyme.

In 2018, Xu et al. [91] reported the design, synthesis, and biological evaluation of a series of pyrimidone derivatives as novel and selective inhibitors of *PfDHODH*. They were based on their previous findings [92] concerning compound 77 that selectively inhibits *PfDHODH* ($IC_{50} = 6$ nM) with >14,000-fold selectivity over *hDHODH* but proved to be less effective *in vivo* due to its poor metabolic properties. Thus, based on a rational drug design through a detailed molecular docking study of 77 in the ubiquinone binding pocket of *PfDHODH*, the authors conceived, synthesized, and studied a novel series of pyrimidone derivatives (Figure 10).

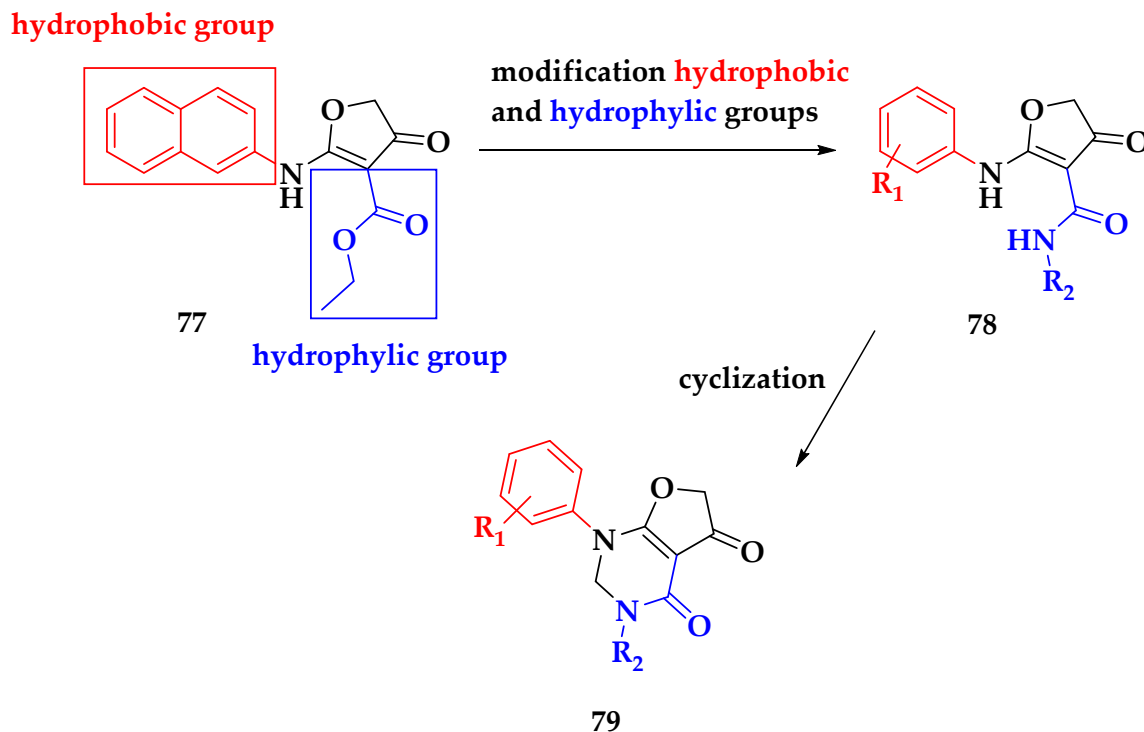
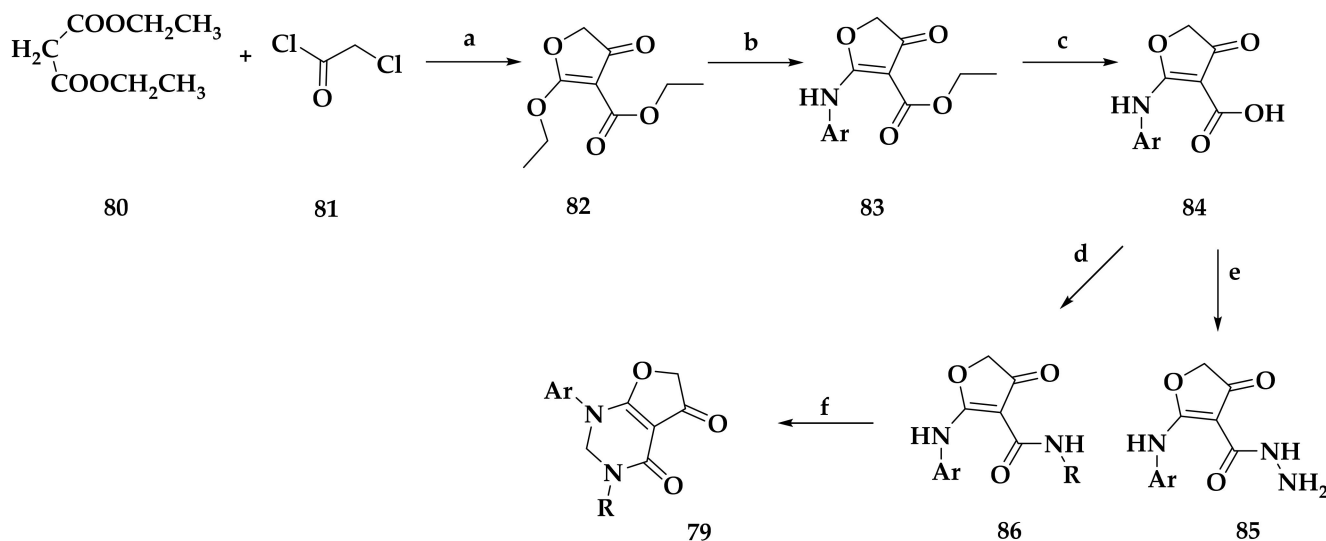


Figure 10. Structural optimization approach of compound 77.

Lactames 79 were synthesized according to Scheme 13. The acid 84 served as a key-synthon for further modifications. It was easily prepared in a 38% overall yield using a known three-step procedure: condensation of diethylmalonate (80) with 2-chloroacetyl chloride (81) followed by substitution of the providing enol ether group with substituted

aniline. Saponification of the ester group followed by a coupling with alkylamines afforded the desired amides **86** in low yields, while reaction of the activated acid with carbonyl-diimidazole and reaction with hydrazine hydrate led to hydrazine-amides **85**, also in low yields.



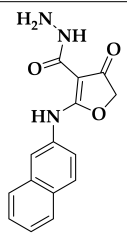
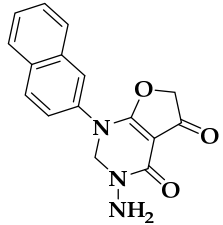
Scheme 13. Synthesis of series of compounds **85** and **79**. Reagents and conditions: (a) NaH, THF, rt to 45 °C to reflux, overnight, 35%; (b) Ar-NH₂; (c) LiOH/H₂O, MeOH/H₂O, 60 °C, 12 h, 80% (two steps); (d) R-NH₂, HOBT/EDC, DIPEA, DCM, rt, overnight, yields 20–25%; (e) 80% hydrazine hydrate, CDI, overnight, rt, 20%; (f) paraformaldehyde, NaOH/EtOH, rt to 70 °C, 9 h, yields 13–20%.

Finally, the authors obtained the rigid six-membered annulated rings by reacting compounds **86** with paraformaldehyde, and subsequent cyclization under basic ethanolic conditions [93] affording compounds **79** in low yields, where two carbonyl groups are pointing in the same direction.

The authors evaluated the inhibitory activities of all synthesized compounds. In the non-annulated series, **86a** emerged as the most active molecule of the series with IC₅₀ = 70 nM. It possesses a 2-naphthyl group and an hydrazinamide function and is slightly more potent than the key intermediate acid which shows the same selectivity against both *h*DHODH and *Pf*DHODH.

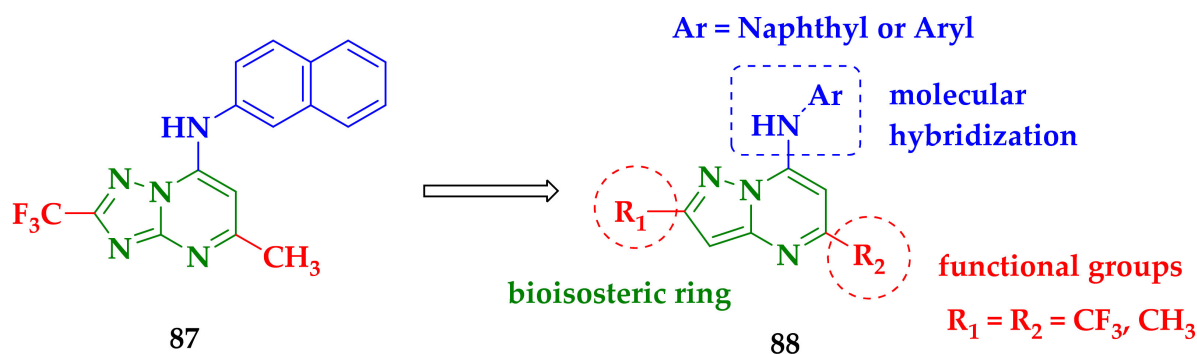
The most active compound among all tested was compound **79a** issued from the annulated series (Table 10). It possesses a 2-naphthyl group, that confers a three-times better activity than compound **86a**, while it is equally selective to *Pf*DHODH/*h*DHODH. The authors obtained an optimal docking pose of compound **79a** based on the X-ray crystal structure of *Pf*DHODH in complex with DSM1 (PDB code 3I65), by applying a flexible induced-fit docking [94] in the ubiquinone binding pocket of *Pf*DHODH. They, thus, were able to show the favorable binding pose of compound **79a**, where the two carbonyl groups of the compound form hydrogen bonds with two important residues into the binding site: Arg265 and His185. The authors also point out the structural stability of compounds **79** in comparison to the non-annulated **86**.

Table 10. *In vitro* results for compounds 86a and 79a.

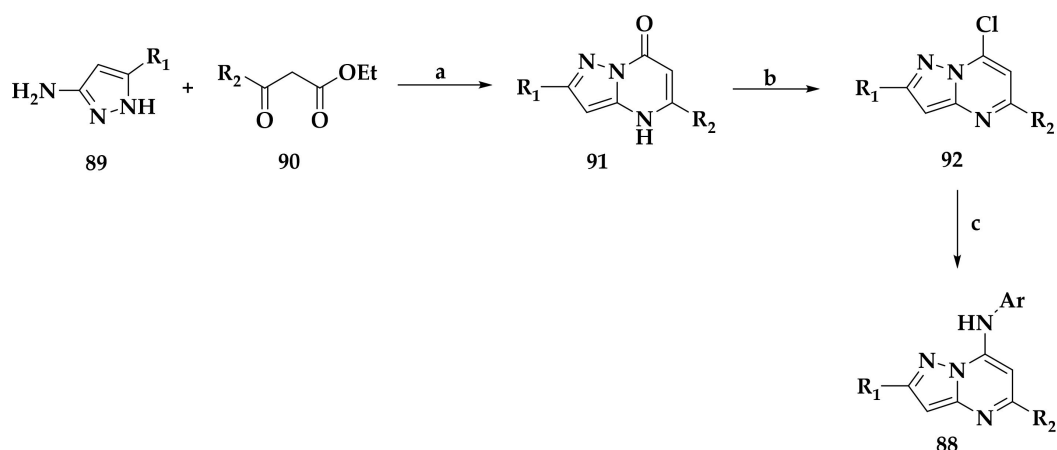
Compound	Structure	IC ₅₀ (μM) <i>Pf</i> DHODH	IC ₅₀ (μM) <i>h</i> DHODH
86a		0.070 ± 0.01	>10
79a		0.023 ± 0.001	>10
DSM1	-	0.042 ± 0.004	-

In 2017, Azeredo et al. reported [95] the synthesis of a series of pyrimidine derivatives and their inhibitory activities against *P. falciparum* and *Pf*DHODH. The same group had already designed, synthesized and evaluated [96] a series of triazolo-trifluoro pyrimidine derivatives and observed the positive influence of the trifluoro group at the C-2 position of the triazolopyrimidine ring on the antiplasmodial activity.

Based on a rational approach and applying a ring bioisosterism replacement (Figure 11), the authors synthesized 15 new compounds in the series of the 7-arylamino pyrazolo-[1,5-a]-pyrimidines, through a straightforward three-step synthetic route depicted in Scheme 14.

**Figure 11.** Rational approach to design molecules 88.

Condensation between 3-aminopyrazoles **89** and the appropriate β -ketoesters **90** provided pyrazolo-[1,5-a]pyrimidinones **91** in 71% and 93% yields. Pyrimidinones **91** were then submitted to a chloro-dehydroxylation [97] in the presence of phosphorous oxychloride leading to chloro-substituted derivatives **92** in 50–82% yields.



Scheme 14. Synthesis of series of compounds **88**. Reagents and conditions: (a) CH_3COOH , reflux, 5–16 h, yields: 71–93%; (b) POCl_3 , 50–82 °C, 1–4 h, yields 50–82%; (c) amine, EtOH or PhMe, 14–26 h, yields 58–81%.

Finally, the reaction of **92** with anilines under aromatic nucleophilic substitution conditions led to the desired derivatives **88** with yields varying between 58% and 81%. The authors performed further molecular docking studies concerning the *Pf*DHODH target (PDB code 3i65) along with redocking studies of the co-crystallized inhibitor JZ8 [98] to validate the selected parameters for their study and evaluate the binding modes of their compounds.

Thirteen, among all compounds tested, were found to be active against *Pf* with IC_{50} values varying between 1.2 ± 0.3 and 92 ± 26 μM , while six of them presented very promising IC_{50} values against *Pf*DHODH. Compounds **88a–c**, were found to be the most relevant with strong activities (6 ± 1 , 4 ± 1 and 0.16 ± 0.01 μM , respectively) and very favorable selectivity indexes (Table 11). The SARs studies showed that the $-\text{CF}_3$ group remains extremely important for the antimalarial activity whether it is introduced at the C-2 or C-5 position. The authors noted that the most active compounds against *Pf*DHODH were found to be the most active ones against *Pf* chloroquine-resistant W2 strain.

Table 11. Determination of cytotoxicity in BGM cell line (MLD_{50}) and IC_{50} values against *Pf*DHODH of selected compounds **88**^a.

Compound	Substituents R_1/R_2	Cytotoxicity (MLD_{50}) (μM)	IC_{50} against <i>Pf</i> DHODH (μM)
88a	2- CF_3 /5- CH_3	561.4 ± 49.7	6 ± 1
88b	2- CH_3 /5- CH_3	406 ± 216	4 ± 1
88c	2- CH_3 /5- CF_3	2341 ± 105	0.16 ± 0.01
87	-	425	0.70 ± 0.08

^a MLD_{50} : minimal lethal dose for 50% of cells.

In 2017, Schreiber et al. reported their efforts to optimize compound **93** (Figure 12) in terms of efficacy against DHODH and *in vivo* [99]. In fact, they were based on their previous findings, where, through conducting a large-scale phenotypic screening of 100,000 already prepared compounds obtained through diverted oriented synthesis [100,101], they identified BRD7539 (**93**), possessing an azetidine 2-carbonitrile core frame, as an inhibitor targeting *Pf*DHODH ($\text{IC}_{50} = 0.033$ μM and SI vs. *h*DHDOH > 150). BRD7539 was also found to be active against both multidrug-resistant asexual blood-stage and liver-stage *P. falciparum*.

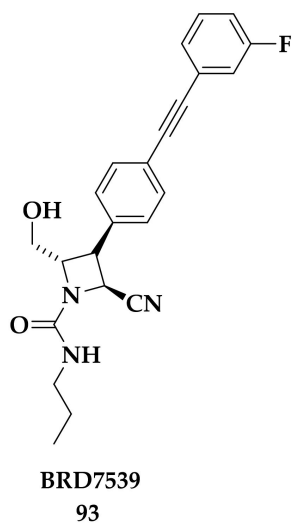
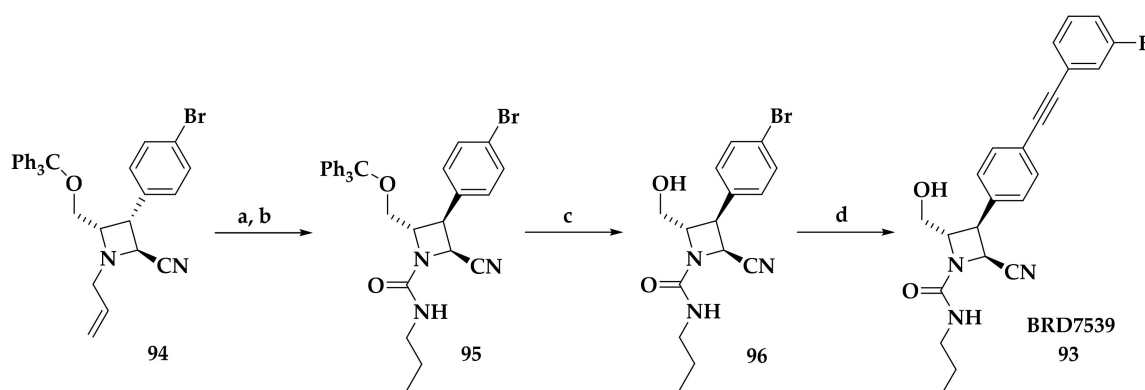


Figure 12. *Pf*DHODH inhibitor BRD7539.

The synthetic route they applied (Scheme 15), makes use of the synthetic strategy of the BRD7539 (93), which was also resynthesized.



Scheme 15. Azetidine-2-carbonitrile scaffold construction. Reagents and conditions: (a) Pd (PPh₃)₄, 1,3-dimethylbarbituric acid, EtOH/DCM (2:1), 40 °C, 16 h, 92%; (b) propylisocyanate, DIPEA, DCM, 23 °C, 1 h, 96%; (c) CF₃COOH, Et₃SiH, DCM, 23 °C, 1 h, 87%; (d) 1-ethynyl-3-fluorobenzene, XPhos, Pd-G3, Et₃N, MeCN, 70 °C, 6 h, 91%.

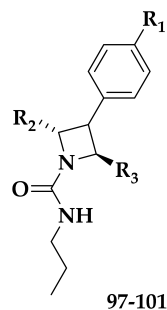
The core structure **94** was obtained as previously reported. De-allylation of the protected azetidine and sequential two-step reaction leads to the urea derivative **95**. Trityl deprotection and Heck alkylation or Suzuki reaction on the brominated phenyl ring of **96** allowed the introduction of many substituents obtained in an overall yield varying between 45% and 55% starting from **94** (Scheme 15).

By using the phenotypic blood-stage growth inhibition assay, the authors showed that the unsubstituted diaryl derivative **97** lacking the acetylenic function that might cause toxicity problems, still possesses an equipotent activity compared to BRD7539 (**93**). However, alkene or alkanes directly linked to the aromatic core group showed a slight loss in activity (Table 12).

The difluorinated derivative **100** was found among the most promising compounds with an EC₅₀ value of 16 nM against multidrug-resistant blood-stage parasites. In addition, the *in vivo* studies showed a curative effect of compound **100** after three doses in a *P. berghei* mouse model, a long life (15 h) and low clearance. Finally, the authors confirmed the target as *Pf*DHODH (IC₅₀ = 12 nM), while for *h*DHODH the IC₅₀ value was 400-fold

bigger ($IC_{50} > 50 \mu M$). They, thus, consider compound **100** a major advance for combating mitochondria targets of malaria (Table 12).

Table 12. EC_{50} values of BRD7539 against Dd2 strains of *P. falciparum*.



Compound	R ₁	R ₂	R ₃	EC ₅₀ (μM)
BRD7539				0.010
97				0.019
98				0.010
99				0.039
100				0.016
101				0.015

3.3. Developing bc1 Antimalarial Inhibitors

In 2018, Okada-Junior et al. reported [102] their study on phthalimide derivatives with activities on *P. falciparum* and targeting the bc1 cytochrome complex. In search of surrogates of atovaquone (Figure 13), the authors described the synthesis and activities of a series of *N*-phenyl substituted phthalimides.

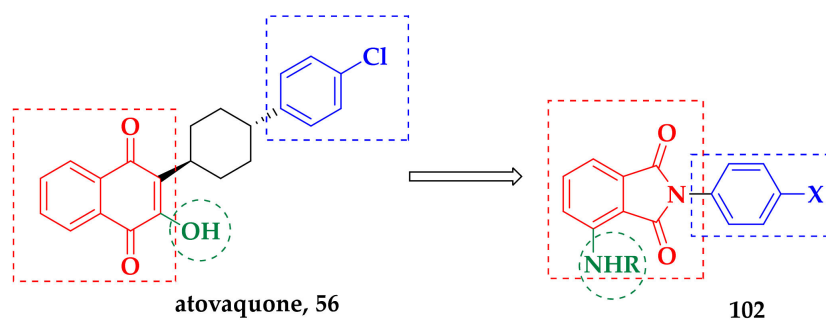
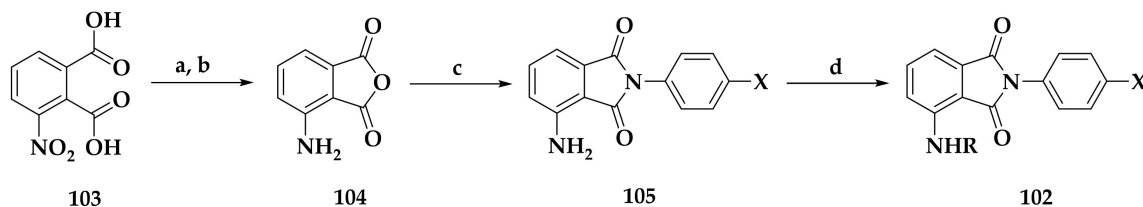


Figure 13. Structural design of the *N*-phenyl phthalimide fragments starting from atovaquone.

The synthetic route developed by the authors is depicted below (Scheme 16). Starting from 3-nitro-phthalic acid (**103**), the anhydride was first obtained followed by catalytic hydrogenation affording 3-aminophthalic anhydride **104**. The latter was then allowed to

react with a variety of appropriate *p*-substituted anilines in glacial acetic acid leading to 3-aminophthalimides **105** that were then functionalized on the amino group affording the desired *N*-benzyl phthalimides **102** in low yields.

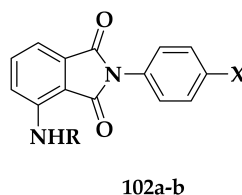


Scheme 16. Synthetic pathway towards *N*-phthalimide derivatives. Reagents and conditions: (a) CH₃COOH, 16 h, reflux, quant.; (b) Pd/C (3%), H₂, 48 h, 80 °C, 57%; (c) CH₃COOH, appropriate *para*-aniline, 7.5 h, reflux, yields 25–80%; (d) R-Br, DMF, 72 h, rt, yields 75–25%.

Among all compounds synthesized and tested, the authors identified derivatives **102a–b** inhibit *P.falciparum* at low micromolar concentrations, indicating the importance of a *p*-OMe substituent. The most active compound of the series **102a** was further investigated showing activity against the multidrug-resistant parasite K1 strain with an IC₅₀ = 4.3 μM.

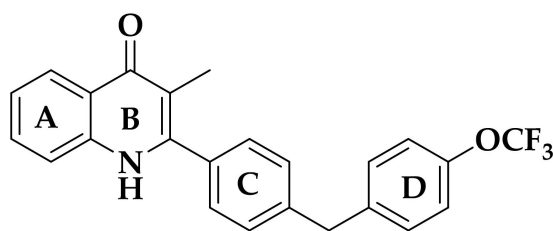
The authors also carried out enzymatic studies to measure the bc1 complex decylubiquinol-cytochrome c oxidoreductase activity, showing that compound **102a** inhibited cytochrome bc1 (74% at 70 μM) (Table 13). Molecular docking studies carried out by using the crystal structure of *S. cerevisiae* cytochrome bc1 complex co-crystallized with stigmatellin [64], were in favor of a most favorable binding of compound **102a** in the Q₀ site of the cytochrome bc1 complex. The authors consider compound **102a** as a new hit for the development of lead compounds targeting the *P. falciparum* mitochondrial bc1 complex.

Table 13. Inhibitory and cytotoxic activities of the derivatives **102a–b** against *P. falciparum* (3D7 strain).



Compound	R/X	% Inhibition at 10 μM	IC ₅₀ (μM)	SI
102a	R = H, X = OMe	75 ± 4	4.2 (3.2–5.2)	>59
102b	R = Bz, X = OMe	65 ± 5	6.8 (5.6–8.0)	>36
artesunate	-	-	0.006 (0.005–0.008)	50.833

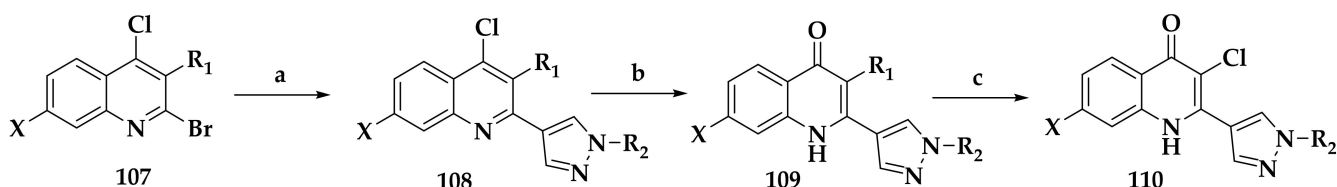
In 2018, Hong et al. [103] reported a series of 2-pyrazolyl quinolone with activities on the bc1 (Qi) complex. They were based on their previous findings [104], where they had already identified compound **106** as one of the lead compounds of a new family (Figure 14). While its physicochemical properties were poor, the authors designed, synthesized and tested a new series of this family of molecules bearing different nitrogen heterocyclic systems in replacement of either C or D rings of **106**.



2-aryl quinolone 106

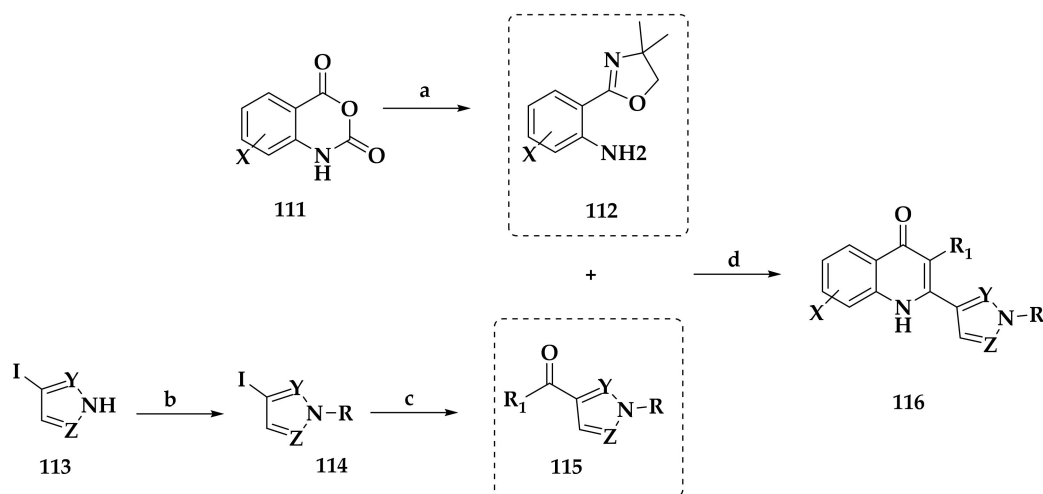
Figure 14. Structure of initial lead compound **106**.

They, thus, prepared two main series of 2-pyrazolyl quinolone analogs by two different synthetic routes. In the first route, 2-bromo 4-chloroquinoline **107** was coupled with pyrazole boronic acid pinacol ester that, upon acid hydrolysis, afforded quinolones **109** in excellent yields (Scheme 17).



Scheme 17. Synthetic pathway towards pyrazole quinolone analogs. Reagents and conditions: (a) pyrazole boronic acid pinacol ester, 10% PdCl₂ (dppf), K₂CO₃·1.5 H₂O, dioxane, 24 h, reflux, yields 36–93%; (b) CH₃COOH, H₂O, 24–48 h, 120 °C or HCl (aq), dioxane, 48 h, reflux or HCOOH/H₂O, DMF, 4 h, 140 °C, yields 47–92%; (c) sodium dichloroisocyanurate, MeOH, NaOH (aq), overnight, rt, yields 56–72%.

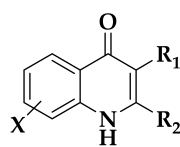
A second family of quinolones, **116**, was elaborated (Scheme 18) by first transforming starting isatoic anhydride **111** to oxazoline **112**. In a parallel step, pyrazoles **113** were synthesized and converted to ketones **115**. Cyclization of oxazolines **112** with ketones **115** under acid-catalyzed conditions afforded the desired quinolones with yields varying between 42% and 84%.



Scheme 18. Synthetic pathway towards pyrazole quinolones **116**. Reagents and conditions: (a) 2-amino-2-methyl-propanol, ZnCl₂, PhCl, 24 h, 135 °C, 60%; (b) appropriate benzyl bromide, K₂CO₃, acetone, 3 h, reflux, yields 65–71%; (c) Pd₂ (dba)₃, dppp, pyrrolidine, mol. sieves, DMF, 6 h, 110 °C, 26–55%; (d) CF₃SO₃H, n-BuOH, N₂, 24 h, 130 °C, yields 42–84%.

Several analogs of the series presented improved *in vitro* antimalarial activities against the 3D7 *P. falciparum* strain in comparison to **106** and IC₅₀ values in the range from 15–33 nM. The authors showed that the most active compounds display improved DMPK properties in terms of solubility and cytotoxicity. By monitoring cytochrome c reduction [105], they also demonstrated that the most active compound, **116d**, targets *Pfbc1*. The authors co-crystallized bovine heart-derived cytochrome bc1 with compound **116b** [106] showing, thus, the binding of the quinolones to the Qi site. They then generated the homology model for the *P. falciparum* cytochrome bc1 complex [107] and performed molecular docking experiments. They, thus, were able to demonstrate (Table 14) the favorable binding of **116b** in the ubiquinone-reducing Qi site of the parasite bc1 complex. Nevertheless, the authors do not exclude the possibility that these compounds target other components of the electron transport chain of the parasite's mitochondrion.

Table 14. *In vitro* antimalarial activities of quinolones against W2 strain of *P. falciparum*.



116a-e

Compound	R ₁ /X	R ₂	IC ₅₀ W2 (nM)
116a	R ₁ = Me, X = H		26
116b	R ₁ = Me, X = H		33
116c	R ₁ = Cl, X = H		14
116d	R ₁ = Cl, X = 7-OMe		11
116e	R ₁ = Me, X = 7-OMe		15
Chloroquine	-	-	12.3
Atovaquone	-	-	0.3

4. Conclusions

The emergence of the resistance to current treatments for malaria has led research groups around the world to increase their efforts to identify new essential biochemical pathways and enzymatic targets where new compounds can be conceived and lead to drug candidates or drugs. It is essential to note that concerning the epigenetics pathways in the *Plasmodium* parasite, as a lot of research has been carried out in relation to other diseases, the actual research is focused on heterocyclic compounds with much better selectivity, pharmacokinetic properties and straightforward synthetic accessibility. *In silico* studies are extremely important to conceive and design compounds with these properties. This domain currently under extensive research seems very promising for developing new antimalarial drugs. The second domain concerning the two specific mitochondria targets presented in this review is also under intense evolution due to the naphthoquinone (and Lawsons's) derivatives and many different heterocyclic scaffolds that could target the bc1 complex and/or the dihydroorotate dehydrogenase. In this domain, where *in silico* studies are still a valuable tool, a lot must still be done, in order to obtain drug candidates in advanced clinical phases.

Author Contributions: Conceptualization, supervision, and organization of the review, M.B.; Bibliography search, C.L.K. and M.B.; Writing—original draft preparation, C.L.K. and M.B.; Corrections, amendments, C.L.K., M.B., A.R. and C.M.A. All authors have read and agreed to the published version of the manuscript.

Funding: The authors gratefully acknowledge the French Ministry of Higher Education and Research for the thesis grant (C.L.K.) and the CNRS, University Paul Sabatier, for financial support.

Institutional Review Board Statement: Not applicable.

Informed Consent Statement: Not applicable.

Data Availability Statement: Not applicable.

Conflicts of Interest: The authors declare no conflict of interest.

References

1. World Health Organization. *World Malaria Report 2020*; World Health Organization: Geneva, Switzerland, 2020.
2. Centers for Disease Control and Prevention. Available online: <https://www.cdc.gov/> (accessed on 3 June 2021).
3. Ledford, H. Malaria vaccine shows promise—Now come tougher trials. *Nature* **2021**, *593*, 17. [[CrossRef](#)]
4. World Health Organization. *Guidelines for the treatment of Malaria*, 3rd ed.; World Health Organization: Geneva, Switzerland, 2015.
5. Blasco, B.; Leroy, D.; Fidock, D.A. Antimalarial drug resistance: Linking *Plasmodium falciparum* parasite biology to the clinic. *Nat. Med.* **2017**, *23*, 917–928. [[CrossRef](#)] [[PubMed](#)]
6. World Health Organization. *Status Report on Artemisinin Resistance and ACT Efficacy*; World Health Organization: Geneva, Switzerland, 2019.
7. Cortés, A.; Crowley, V.M.; Vaquero, A.; Voss, T.S.; Rall, G.F. A View on the Role of Epigenetics in the Biology of Malaria Parasites. *PLoS Pathog.* **2012**, *8*, e1002943. [[CrossRef](#)] [[PubMed](#)]
8. Krungkrai, J. The multiple roles of the mitochondrion of the malarial parasite. *Parasitology* **2004**, *129*, 511–524. [[CrossRef](#)]
9. Vaidya, A.B.; Mather, M.W. Mitochondrial Evolution and Functions in Malaria Parasites. *Annu. Rev. Microbiol.* **2009**, *63*, 249–267. [[CrossRef](#)]
10. Gupta, A.P.; Chin, W.H.; Zhu, L.; Mok, S.; Luah, Y.H.; Lim, E.H.; Bozdech, Z. Dynamic Epigenetic Regulation of Gene Expression during the Life Cycle of Malaria Parasite *Plasmodium falciparum*. *PLoS Pathog.* **2013**, *9*, e1003170. [[CrossRef](#)] [[PubMed](#)]
11. Malmquist, N.A.; Sundriyal, S.; Caron, J.; Chen, P.; Witkowski, B.; Menard, D.; Suwanarusk, R.; Renia, L.; Nosten, F.; Jiménez-Díaz, M.B.; et al. Histone Methyltransferase Inhibitors Are Orally Bioavailable, Fast-Acting Molecules with Activity against Different Species Causing Malaria in Humans. *Antimicrob. Agents Chemother.* **2015**, *59*, 950–959. [[CrossRef](#)] [[PubMed](#)]
12. Ponts, N.; Fu, L.; Harris, E.Y.; Zhang, J.; Chung, D.W.D.; Cervantes, M.C.; Prudhomme, J.; Atanasova-Penichon, V.; Zehraoui, E.; Bunnik, E.M.; et al. Genome-wide mapping of DNA methylation in the human malaria parasite *Plasmodium falciparum*. *Cell Host Microbe*. **2013**, *14*, 696–706. [[CrossRef](#)]
13. Hammam, E.; Ananda, G.; Sinha, A.; Scheidig-Benatar, C.; Bohec, M.; Preiser, P.R.; Dedon, P.C.; Scherf, A.; Vembar, S.S. Discovery of a new predominant cytosine DNA modification that is linked to gene expression in malaria parasites. *Nucleic Acids Res.* **2020**, *48*, 184–199. [[CrossRef](#)] [[PubMed](#)]
14. Coetzee, N.; von Grüning, H.; Opperman, D.; van der Watt, M.; Reader, J.; Birkholtz, L.R. Epigenetic inhibitors target multiple stages of *Plasmodium falciparum* parasites. *Sci. Rep.* **2020**, *10*, 2355. [[CrossRef](#)]

15. Ngwa, C.J.; Gross, M.R.; Musabyimana, J.P.; Pradel, G.; Deitsch, K.W. The Role of The Histone Methyltransferase PfSET10 in Antigenic Variation by Malaria Parasites: A Cautionary Tale. *mSphere* **2021**, *6*, e01217-20. [[CrossRef](#)]
16. Chan, A.; Dziedzic, A.; Kirkman, L.A.; Deitsch, K.W.; Ankarklev, J. A histone methyltransferase inhibitor can reverse epigenetically acquired drug resistance in the malaria parasite *Plasmodium falciparum*. *Antimicrob. Agents Chemother.* **2020**, *64*, e02021-19. [[CrossRef](#)]
17. Fioravanti, R.; Mautone, N.; Rovere, A.; Rotili, D.; Mai, A. Targeting histone acetylation/deacetylation in parasites: An update (2017–2020). *Curr. Opin. Chem. Biol.* **2020**, *57*, 65–74. [[CrossRef](#)]
18. Bouchut, A.; Rotili, D.; Pierrot, C.; Valente, S.; Lafitte, S.; Schultz, J.; Høglund, U.; Mazzone, R.; Lucidi, A.; Fabrizi, G.; et al. Identification of novel quinazoline derivatives as potent antiplasmodial agents. *Eur. J. Med. Chem.* **2019**, *161*, 277–291. [[CrossRef](#)] [[PubMed](#)]
19. Halby, L.; Menon, Y.; Rilova, E.; Pechalrieu, D.; Masson, V.; Faux, C.; Bouhleb, M.A.; David-Cordonnier, M.H.; Novosad, N.; Aussagues, Y.; et al. Rational Design of Bisubstrate-Type Analogs as Inhibitors of DNA Methyltransferases in Cancer Cells. *J. Med. Chem.* **2017**, *60*, 4665–4679. [[CrossRef](#)] [[PubMed](#)]
20. Nardella, F.; Halby, L.; Hammam, E.; Erdmann, D.; Cadet-Daniel, V.; Peronet, R.; Meñard, D.; Witkowski, B.; Mecheri, S.; Scherf, A.; et al. DNA Methylation Bisubstrate Inhibitors Are Fast-Acting Drugs Active against Artemisinin-Resistant *Plasmodium falciparum* Parasites. *ACS Cent. Sci.* **2020**, *6*, 16–21. [[CrossRef](#)]
21. Buchini, S.; Leumann, C. 2-O'-Aminoethyl Oligoribonucleotides Containing Novel Base Analogs: Synthesis and Triple-Helix Formation at Pyrimidine/Purine Inversion Sites. *Eur. J. Org. Chem.* **2006**, 3152–3168. [[CrossRef](#)]
22. Philips, D.M. The presence of acetyl groups of histones. *Biochem. J.* **1963**, *87*, 258–263. [[CrossRef](#)] [[PubMed](#)]
23. Allfrey, V.G.; Faulkner, R.; Mirsky, A.E. Acetylation and Methylation of Histones and Their Possible Role in the Regulation of RNA Synthesis. *Proc. Natl. Acad. Sci. USA* **1964**, *51*, 786–794. [[CrossRef](#)]
24. Benedetti, R.; Conte, M.; Altucci, L. Targeting histone deacetylases in diseases: Where are we? *Antioxid. Redox. Signal.* **2015**, *23*, 99–126. [[CrossRef](#)]
25. Mann, B.S.; Johnson, J.R.; Cohen, M.H.; Justice, R.; Pazdur, R. FDA approval summary: Vorinostat for treatment of advanced primary cutaneous T-cell lymphoma. *Oncologist* **2007**, *12*, 1247–1252. [[CrossRef](#)] [[PubMed](#)]
26. Moore, D. Panobinostat (Farydak): A novel option for the treatment of relapsed or relapsed and refractory multiple myeloma. *Pharm. Ther.* **2016**, *41*, 296–300.
27. Lee, H.Z.; Kwitkowski, V.E.; Del Valle, P.L.; Ricci, M.S.; Saber, H.; Habtemariam, B.A.; Bullock, J.; Bloomquist, E.; Li Shen, Y.; Chen, X.H.; et al. FDA approval: Belinostat for the treatment of patients with relapsed or refractory peripheral T-cell lymphoma. *Clin. Cancer. Res.* **2015**, *21*, 2666–2670. [[CrossRef](#)] [[PubMed](#)]
28. Barbarotta, L.; Hurley, K. Romidepsin for the treatment of peripheral T-cell lymphoma. *J. Adv. Pract. Oncol.* **2015**, *6*, 22–36. [[CrossRef](#)] [[PubMed](#)]
29. Ganesan, A.; Arimondo, P.B.; Rots, M.G.; Jeronimo, C.; Berdasco, M. The Timeline of Epigenetic Drug Discovery: From Reality to Dreams. *Clin. Epigenet.* **2019**, *11*, 174–190. [[CrossRef](#)]
30. Morales Torres, C.; Wu, M.Y.; Hobor, S.; Wainwright, E.N.; Martin, M.J.; Patel, H.; Grey, W.; Grönroos, E.; Howell, S.; Carvalho, J.; et al. Selective inhibition of cancer cell self-renewal through a Quisinostat-histone H1.0 axis. *Nat. Commun.* **2020**, *11*, 1792–1807. [[CrossRef](#)]
31. Engel, J.A.; Jones, A.J.; Avery, V.M.; Sumanadasa, S.D.M.; Ng, S.S.; Fairlie, D.P.; Adams, T.S.; Skinner-Adams, K.T. Profiling the anti-protozoal activity of anti-cancer HDAC inhibitors against *Plasmodium* and *Trypanosoma* parasites. *Int. J. Parasitol. Drug. Resist.* **2015**, *5*, 117–126. [[CrossRef](#)]
32. Andrews, K.T.; Gupta, A.P.; Tran, T.N.; Fairlie, D.P.; Gobert, G.N.; Bozdhek, Z. Comparative gene expression profiling of *P. falciparum* malaria parasites exposed to three different histone deacetylase inhibitors. *PLoS ONE* **2012**, *7*, e31847. [[CrossRef](#)]
33. Andrews, K.T.; Tran, T.N.; Wheatley, N.C.; Fairlie, D.P. Targeting Histone Deacetylase Inhibitors for Anti-Malarial Therapy. *Curr. Top. Med. Chem.* **2009**, *9*, 292–308. [[CrossRef](#)]
34. Darkin-Rattray, S.J.; Gurnett, A.M.; Myers, R.W.; Dulski, P.M.; Crumley, T.M.; Allocco, J.J.; Cannova, C.; Meinke, P.T.; Colletti, S.L.; Bednarek, M.A.; et al. Apicidin: A Novel Antiprotozoal Agent that Inhibits Parasite Histone Deacetylase. *Proc. Natl. Acad. Sci. USA* **1996**, *93*, 13143–13147. [[CrossRef](#)] [[PubMed](#)]
35. Andrews, K.; Tran, T.N.; Fairlie, D.P. Towards Histone Deacetylase Inhibitors as New Antimalarial Drugs. *Curr. Pharm. Des.* **2012**, *18*, 3467–3479. [[CrossRef](#)] [[PubMed](#)]
36. Ontoria, J.M.; Paonessa, G.; Ponzi, S.; Ferrigno, F.; Nizi, E.; Biancofiore, I.; Malancona, S.; Graziani, R.; Roberts, D.; Willis, P.; et al. Discovery of a Selective Series of Inhibitors of *Plasmodium falciparum* HDACs. *ACS Med. Chem. Lett.* **2016**, *7*, 454–459. [[CrossRef](#)] [[PubMed](#)]
37. Atenni, B.; Ferrigno, F.; Jones, P.; Ingenito, R.; Kinzel, O.; Llauger-Bufi, L.; Ontoria, J.M.; Pescatore, G.; Rowley, M.; Scarpelli, R.; et al. Heterocycles Derivatives as Histone Deacetylase (HDAC) Inhibitors. WO/2006/061638, 15 June 2006.
38. Deziel, R.; Rahil, J.; Wahhab, A.; Allan, M.; Nguyen, N. Sirtuin Inhibitors. WO/2009/026701, 3 March 2009.
39. Mackwitz, M.K.W.; Hespings, E.; Antonova-Koch, Y.; Diedrich, D.; Woldearegai, T.G.; Skinner-Adams, T.; Clarke, M.; Schöler, A.; Limbach, L.; Kurz, T.; et al. Structure-Activity and Structure-Toxicity Relationships of Peptoid-Based Histone Deacetylase Inhibitors with Dual-Stage Antiplasmodial Activity. *Chem. Med. Chem.* **2019**, *14*, 912–926. [[CrossRef](#)]

40. Andrews, K.T.; Tran, T.N.; Lucke, A.J.; Kahnberg, P.; Le, G.T.; Boyle, G.M.; Gardiner, D.L.; Skinner-Adams, T.S.; Fairlie, D.P. Potent antimalarial activity of histone deacetylase inhibitor analogs. *Antimicrob. Agents Chemother.* **2008**, *52*, 1454–1461. [[CrossRef](#)] [[PubMed](#)]
41. Chua, M.J.; Arnold, M.S.J.; Xu, W.; Lancelot, J.; Lamotte, S.; Späth, G.F.; Prina, E.; Pierce, R.J.; Fairlie, D.P.; Skinner-Adams, T.S.; et al. Effect of clinically approved HDAC inhibitors on *Plasmodium*, *Leishmania* and *Schistosoma* parasite growth. *Int. J. Parasitol. Drugs Drug Resist.* **2017**, *7*, 42–50. [[CrossRef](#)]
42. Melesina, J.; Robaa, D.; Pierce, R.J.; Romier, C.; Sippl, W. Homology modeling of parasite histone deacetylases to guide the structure-based design of selective inhibitors. *J. Mol. Graphics Modell.* **2015**, *62*, 342–361. [[CrossRef](#)]
43. Hailu, G.S.; Robaa, D.; Forgione, M.; Sippl, W.; Rotili, D.; Mai, A. Lysine Deacetylase Inhibitors in Parasites: Past, Present, and Future Perspectives. *J. Med. Chem.* **2017**, *60*, 4780–4804. [[CrossRef](#)]
44. Diedrich, D.; Stenzel, K.; Hespings, E.; Antonova-Koch, Y.; Geburu, T.; Duffy, S.; Fisher, G.; Schçler, A.; Meister, S.; Kurz, T.; et al. One-pot, multi-component synthesis and structure-activity relationships of peptoid-based histone deacetylase (HDAC) inhibitors targeting malaria parasites. *Eur. J. Med. Chem.* **2018**, *158*, 801–813. [[CrossRef](#)]
45. Li, R.; Ling, D.; Tang, T.; Huang, Z.; Wang, M.; Ding, Y.; Liu, T.; Wei, H.; Xu, W.; Mao, F.; et al. Discovery of Novel *Plasmodium falciparum* HDAC1 Inhibitors with Dual-Stage Antimalarial Potency and Improved Safety Based on the Clinical Anticancer Drug Candidate Quisinostat. *J. Med. Chem.* **2021**, *64*, 2254–2271. [[CrossRef](#)]
46. Jiang, L.; Haung, Z. Novel High-Efficiency Antimalarial Drug, Quisinostat. WO/2017/143964, 31 August 2017.
47. Zheng, Y.; Tice, C.M.; Singh, S.B. The Use of Spirocyclic Scaffolds in Drug Discovery. *Bioorg. Med. Chem. Lett.* **2014**, *24*, 3673–3682. [[CrossRef](#)]
48. Dickens, J.W.J.; Houpis, I.N.; Lang, Y.L.; Leys, C.; Stokbroekx, S.C.M.; Weerts, J.E.E. Mono-Hydrochloric Salts of an Inhibitor of Histone Deacetylase. WO2008138918A1, 20 November 2008.
49. Nardella, F.; Halby, L.; Dobrescu, I.; Viluma, J.; Bon, J.; Claes, A.; Cadet-Daniel, V.; Tafit, A.; Roesch, C.; Hammam, E.; et al. Procainamide–SAHA Fused Inhibitors of *h*HDAC6 Tackle Multidrug-Resistant Malaria Parasites. *J. Med. Chem.* **2021**, *64*, 10403–10417. [[CrossRef](#)] [[PubMed](#)]
50. Lee, B.H.; Yegnasubramanian, S.; Lin, X.; Nelson, W.G. Procainamide Is a Specific Inhibitor of DNA Methyltransferase 1. *J. Biol. Chem.* **2005**, *280*, 40749–40756. [[CrossRef](#)] [[PubMed](#)]
51. Kumar, A.; Dhar, S.K.; Subbarao, N. In silico identification of inhibitors against *Plasmodium falciparum* histone deacetylase 1 (PfHDAC-1). *J. Mol. Model.* **2018**, *24*, 232. [[CrossRef](#)] [[PubMed](#)]
52. Webb, B.; Sali, A. Protein structure modeling with MODELLER. *Methods Mol. Biol.* **2014**, *1137*, 1–15. [[CrossRef](#)]
53. Singh, A.; Maqbool, M.; Mobashir, M.; Hoda, N. Dihydroorotate dehydrogenase: An inevitable drug target for the development of antimalarials. *Eur. J. Med. Chem.* **2017**, *125*, 640–651. [[CrossRef](#)]
54. Murphy, M.P.; Hartley, R.C. Mitochondria as a therapeutic target for common pathologies. *Nat. Rev. Drug Discov.* **2018**, *12*, 865–886. [[CrossRef](#)]
55. Berry, E.A.; Huang, L.S.; Saechao, L.K.; Pon, N.G.; Valkova-Valchanova, M.; Daldal, F. X-ray structure of *Rhodobacter capsulatus* cytochrome bc1: Comparison with its mitochondrial and chloroplast counterparts. *Photosynth. Res.* **2004**, *81*, 251–275. [[CrossRef](#)] [[PubMed](#)]
56. Hunte, C.; Koepke, J.; Lange, C.; Rossmann, T.; Michel, H. Structure at 2.3 Å resolution of the cytochrome bc1 complex from the yeast *Saccharomyces cerevisiae* co-crystallized with an antibody Fv fragment. *Structure* **2000**, *8*, 669–684. [[CrossRef](#)]
57. Xia, D.; Yu, C.A.; Kim, H.; Xia, J.Z.; Kachurin, A.M.; Zhang, L.; Yu, L.; Deisenhofer, J. Crystal Structure of the Cytochrome bc1 Complex from Bovine Heart Mitochondria. *Science* **1997**, *277*, 60–66. [[CrossRef](#)] [[PubMed](#)]
58. Zhang, Z.; Huang, L.; Shulmeister, V.M.; Chi, Y.L.; Kim, K.K.; Hung, L.W.; Crofts, A.R.; Berry, E.A.; Kim, S.H. Electron transfer by domain movement in cytochrome bc1. *Nature* **1998**, *392*, 677–684. [[CrossRef](#)] [[PubMed](#)]
59. Yang, X.; Trumpower, B.L. Purification of a three-subunit ubiquinol-cytochrome c oxidoreductase complex from *Paracoccus denitrificans*. *J. Biol. Chem.* **1986**, *261*, 12282–12289. [[CrossRef](#)]
60. Mitchell, P. Possible molecular mechanisms of the protonmotive function of cytochrome systems. *J. Theor. Biol.* **1976**, *62*, 327–367. [[CrossRef](#)]
61. Erecińska, M.; Chance, B.; Wilson, D.F.; Dutton, P.L. Aerobic Reduction of Cytochrome b566 in Pigeon-Heart Mitochondria. *Proc. Natl. Acad. Sci. USA* **1972**, *69*, 50–54. [[CrossRef](#)] [[PubMed](#)]
62. Huang, L.S.; Cobessi, D.; Tung, E.Y.; Berry, E.A. Binding of the Respiratory Chain Inhibitor Antimycin to the Mitochondrial bc1 Complex: A New Crystal Structure Reveals an Altered Intramolecular Hydrogen-bonding Pattern. *J. Mol. Biol.* **2005**, *351*, 573–597. [[CrossRef](#)] [[PubMed](#)]
63. Hao, G.F.; Wang, F.; Li, H.; Zhu, X.L.; Yang, W.C.; Huang, L.S.; Wu, J.W.; Berry, E.A.; Yang, G.F. Computational Discovery of Picomolar Qo Site Inhibitors of Cytochrome bc1 Complex. *J. Am. Chem. Soc.* **2012**, *134*, 11168–11176. [[CrossRef](#)]
64. Solmaz, S.R.N.; Hunte, C. Structure of complex III with bound cytochrome c in reduced state and definition of a minimal core interface for electron transfer. *J. Biol. Chem.* **2008**, *283*, 17542–17549. [[CrossRef](#)]
65. Esser, L.; Elberry, M.; Zhou, F.; Yu, C.A.; Yu, L.; Xia, D. Inhibitor-complexed Structures of the Cytochrome bc1 from the Photosynthetic Bacterium *Rhodobacter sphaeroides*. *J. Biol. Chem.* **2008**, *283*, 2846–2857. [[CrossRef](#)]
66. Painter, H.J.; Morrissey, J.M.; Mather, M.W.; Vaidya, A.B. Specific role of mitochondrial electron transport in blood-stage *Plasmodium falciparum*. *Nature* **2007**, *446*, 88–91. [[CrossRef](#)] [[PubMed](#)]

67. Fagan, R.L.; Nelson, M.N.; Pagano, P.M.; Palfey, B.A. Mechanism of Flavin Reduction in Class 2 Dihydroorotate Dehydrogenases. *Biochemistry* **2006**, *45*, 14926–14932. [CrossRef]
68. Phillips, M.A.; Rathod, P.K. *Plasmodium* dihydroorotate dehydrogenase: A promising target for novel anti-malarial chemotherapy. *Infect. Disord. Drug Targets* **2010**, *10*, 226–239. [CrossRef]
69. Coteron, J.M.; Marco, M.A.; Esquivias, J.; Deng, X.; White, K.L.; White, J.; Koltun, M.; El Mazouni, F.; Kokkonda, S.; Katneni, K.; et al. Structure-Guided Lead Optimization of Triazolopyrimidine-Ring Substituents Identifies Potent *Plasmodium falciparum* Dihydroorotate Dehydrogenase Inhibitors with Clinical Candidate Potential. *J. Med. Chem.* **2011**, *54*, 5540–5561. [CrossRef] [PubMed]
70. Fry, M.; Pudney, M. Site of action of the antimalarial hydroxynaphthoquinone, 2-[trans-4-(4'-chlorophenyl)cyclohexyl]-3-hydroxy-1,4-naphthoquinone (566C80). *Biochem. Pharmacol.* **1992**, *43*, 1545–1553. [CrossRef]
71. Shanks, G.D.; Gordon, D.M.; Klotz, F.W.; Aleman, G.M.; Oloo, A.J.; Sadie, D.; Scott, T.R. Efficacy and Safety of Atovaquone/Proguanil as Suppressive Prophylaxis for *Plasmodium falciparum* Malaria. *Clin. Infect. Dis.* **1998**, *27*, 494–499. [CrossRef]
72. Srivastava, I.K.; Morrisey, J.M.; Darrouzet, E.; Daldal, F.; Vaidya, A.B. Resistance mutations reveal the atovaquone-binding domain of cytochrome b in malaria parasites. *Mol. Microbiol.* **1999**, *33*, 704–711. [CrossRef]
73. Srivastava, I.K.; Vaidya, A.B. A mechanism for the Synergistic Antimalarial Action of Atovaquone and Proguanil. *Antimicrob. Agents Chemother.* **1999**, *43*, 1334–1339. [CrossRef] [PubMed]
74. Birth, D.; Kao, W.C.; Hunte, C. Structural analysis of atovaquone-inhibited cytochrome bc1 complex reveals the molecular basis of antimalarial drug action. *Nat. Commun.* **2014**, *5*, 4029. [CrossRef] [PubMed]
75. Hudson, A.T.; Randall, A.W. Naphthoquinone derivatives. U.S. Patent 5053432A, 1 October 1991.
76. Hudson, A.T.; Latter, V. Medicaments. EP0580185A1, 26 January 1994.
77. Antonio, N.; Mara, S.; Annibale, S.; Stefan, M. Process for the preparation of trans-2,3-disubstituted naphthoquinones. U.S. Patent 7,842,840 B2. 2010. *Chem. Abstr.* **2008**, *149*, 576277.
78. Saralya, S.S.; Shasikumar, S.H.; Shashipraba, S.; Kanakamajalu, S.; Koottungalamadhom, R.R.; Ananathalakshmi, V.; Govindarajalu, J.; Rao, K.S.; Nagarajan, K. Preparation of naphthoquinone compounds using 2,3-dihalonaphthoquinone. WO 2009122432A2, 8 October 2009.
79. Williams, D.R.; Clark, M.P. Synthesis of atovaquone. *Tetrahedron Lett.* **1998**, *39*, 7629–7632. [CrossRef]
80. Dwyer, A.N.; Gordon, A.; Urquhart, M. Novel process. WO/2012/080243 A2, 21 June 2012.
81. Britton, H.; Catterick, D.; Dwyer, A.N.; Gordon, A.H.; Leach, S.G.; McCormick, C.; Mountain, C.E.; Simpson, A.; Stevens, D.R.; Urquhart, M.W.J.; et al. Discovery and Development of an Efficient Process to Atovaquone. *Org. Process Res. Dev.* **2012**, *16*, 1607–1617. [CrossRef]
82. Dike, S.Y.; Singh, D.; Thankachen, B.N.; Sharma, B.; Mathur, P.K.; Kore, S.; Kumar, A. A Single-Pot Synthesis of Atovaquone: An Antiparasitic Drug of Choice. *Org. Process Res. Dev.* **2014**, *18*, 618–625. [CrossRef]
83. Borgati, T.F.; Alves do Nascimento, M.F.; Bernardino, J.F.; Oliveira Martins, L.C.; Gutterres Taranto, A.; Braga de Oliveira, A. Synthesis, SAR, and Docking Studies Disclose 2-Arylfuran-1,4-naphthoquinones as In Vitro Antiplasmodial Hits. *J. Trop. Med.* **2017**, *2017*, 7496934. [CrossRef]
84. Nogueira, F.; Rosário, V.E. Methods for assessment of antimalarial activity in the different phases of the *Plasmodium* life cycle. *Rev. Pan-Amaz. Saude* **2010**, *3*, 109–124. [CrossRef]
85. Makler, M.T.; Piper, R.C.; Milhous, W.K. Lactate dehydrogenase and the diagnosis of malaria. *Parasitol. Today* **1998**, *9*, 376–377. [CrossRef]
86. Kapadia, G.J.; Azuine, M.A.; Balasubramanian, V.; Sridhar, R. Amino-naphthoquinones—a novel class of compounds with potent antimalarial activity against *Plasmodium falciparum*. *Pharmacol. Res.* **2001**, *4*, 363–367. [CrossRef] [PubMed]
87. Oramas-Royo, S.; López-Rojas, P.; Amesty, A.; Gutiérrez, D.; Flores, N.; Martín-Rodríguez, P.; Fernández-Pérez, L.; Estévez-Braun, A. Synthesis and Antiplasmodial Activity of 1,2,3-Triazole-Naphthoquinone Conjugates. *Molecules* **2019**, *24*, 3917. [CrossRef]
88. Rostovtsev, V.V.; Green, L.G.; Fokin, V.V.; Sharpless, K.B. A Stepwise Huisgen Cycloaddition Process: Copper(I)-Catalyzed Regioselective “Ligation” of Azides and Terminal Alkynes. *Angew. Chem. Int. Ed.* **2002**, *41*, 2596–2599. [CrossRef]
89. Hurt, D.E.; Widom, J.; Clardy, J. Structure of *Plasmodium falciparum* dihydroorotate dehydrogenase with a bound inhibitor. *Acta Cryst.* **2006**, *62*, 312–323. [CrossRef]
90. Deng, X.; Matthews, D.; Rathod, P.K.; Phillips, M.A. The X-ray structure of *Plasmodium falciparum* dihydroorotate dehydrogenase bound to a potent and selective N-phenylbenzamide inhibitor reveals novel binding-site interactions. *Acta Cryst. Sect. F Struct. Biol. Commun.* **2015**, *71*, 553–559. [CrossRef] [PubMed]
91. Xu, L.; Li, W.; Diao, Y.; Sun, H.; Li, H.; Zhu, L.; Zhou, H.; Zhao, Z. Synthesis, Design, and Structure–Activity Relationship of the Pyrimidone Derivatives as Novel Selective Inhibitors of *Plasmodium falciparum* Dihydroorotate Dehydrogenase. *Molecules* **2018**, *23*, 1254. [CrossRef] [PubMed]
92. Xu, M.; Zhu, J.; Diao, Y.; Zhou, H.; Ren, X.; Sun, D.; Huang, J.; Han, D.; Zhao, Z.; Zhu, L.; et al. Novel selective and potent inhibitors of malaria parasite dihydroorotate dehydrogenase: Discovery and optimization of dihydrothiophenone derivatives. *J. Med. Chem.* **2013**, *56*, 7911–7924. [CrossRef]
93. Knecht, W.; Henseling, J.; Löffler, M. Kinetics of Inhibition of Human and Rat Dihydroorotate Dehydrogenase by Atovaquone, Lawsone Derivatives, Brequinar Sodium and Polyporic Acid. *Chem. Biol. Interact.* **2000**, *124*, 61–76. [CrossRef]

94. Woody, S.; Tyler, D.; Matthew, P.J.; Richard, A.F.; Ramy, F. Novel Procedure for Modeling Ligand/Receptor Induced Fit Effects. *J. Med. Chem.* **2006**, *49*, 534–553. [[CrossRef](#)]
95. Azeredo, L.F.S.P.; Coutinho, J.P.; Jabor, V.A.P.; Feliciano, P.R.; Nonato, M.R.; Kaiser, C.R.; Menezes, C.M.S.; Hammes, A.S.O.; Cafarella, E.R.; Hoelz, L.V.B.; et al. Evaluation of 7-arylaminopyrazolo[1,5-a]pyrimidines as anti-*Plasmodium falciparum*, antimalarial, and *Pf*-dihydroorotate dehydrogenase inhibitors. *Eur. J. Med. Chem.* **2017**, *126*, 72–83. [[CrossRef](#)] [[PubMed](#)]
96. Boechat, N.; Pinheiro, L.C.S.; Silva, T.S.; Aguiar, A.C.C.; Carvalho, A.S.; Bastos, M.M.; Costa, C.C.P.; Pinheiro, S.; Pinto, A.C.; Mendonça, J.S.; et al. New trifluoromethyl triazolopyrimidines as anti-*Plasmodium falciparum* agents. *Molecules* **2012**, *17*, 8285–8302. [[CrossRef](#)] [[PubMed](#)]
97. Senga, K.; Novinson, T.; Wilson, H.R. Synthesis and Antischistosomal activity of certain Pyrazolo[1,5-a]pyrimidines. *J. Med. Chem.* **1981**, *24*, 610–613. [[CrossRef](#)] [[PubMed](#)]
98. Morris, G.M.; Goodsell, D.S.; Halliday, R.S.; Huey, R.; Hart, W.E.; Belew, R.K.; Olson, A.J. Automated docking using a Lamarckian genetic algorithm and empirical binding free energy function. *J. Comput. Chem.* **1998**, *19*, 1639–1662. [[CrossRef](#)]
99. Maetani, M.; Kato, N.; Jabor, V.A.P.; Calil, F.A.; Nonato, M.C.; Scherer, C.A.; Schreiber, S.L. Discovery of Antimalarial Azetidine-2-carbonitriles That Inhibit *P. falciparum* Dihydroorotate Dehydrogenase. *ACS Med. Chem. Lett.* **2017**, *8*, 438–442. [[CrossRef](#)]
100. Kato, N.; Comer, E.; Sakata-Kato, T.; Sharma, A.; Sharma, M.; Maetani, M.; Bastien, J.; Brancucci, N.M.; Bittker, J.A.; Corey, V.; et al. Diversity-oriented synthesis yields novel multistage antimalarial inhibitors. *Nature* **2016**, *538*, 344–349. [[CrossRef](#)]
101. Dancík, V.; Seiler, K.P.; Young, D.W.; Schreiber, S.L.; Clemons, P.A. Distinct biological network properties between the targets of natural products and disease genes. *J. Am. Chem. Soc.* **2010**, *132*, 9259–9261. [[CrossRef](#)]
102. Okada-Junior, C.Y.; Monteiro, G.C.; Campos Aguiar, A.N.; Batista, V.S.; Oliveira de Souza, J.; Souza, G.E.; Bueno, R.V.; Oliva, G.; Nascimento-Júnior, N.M.; Victorio, R.; et al. Phthalimide Derivatives with Bioactivity against *Plasmodium falciparum*: Synthesis, Evaluation, and Computational Studies Involving bc1 Cytochrome Inhibition. *ACS Omega* **2018**, *3*, 9424–9430. [[CrossRef](#)]
103. Hong, W.D.; Leung, S.C.; Ampornnanai, K.; Davies, J.; Priestley, R.S.; Nixon, G.L.; Berry, N.G.; Hasnain, S.S.; Antonyuk, S.; Ward, S.A.; et al. Potent Antimalarial 2-Pyrazolyl Quinolone bc1 (Qi) Inhibitors with Improved Drug-like Properties. *ACS Med. Chem. Lett.* **2018**, *9*, 1205–1210. [[CrossRef](#)] [[PubMed](#)]
104. Pidathala, C.; Amewu, R.; Pacorel, B.; Nixon, G.L.; Gibbons, P.; Hong, W.D.; Leung, S.C.; Berry, N.G.; Sharma, R.; Stocks, P.A.; et al. Identification, Design and Biological Evaluation of Bisaryl Quinolones Targeting *Plasmodium falciparum* Type II NADH: Quinone Oxidoreductase (*Pf*NDH2). *J. Med. Chem.* **2012**, *55*, 1831–1843. [[CrossRef](#)] [[PubMed](#)]
105. Biagini, G.A.; Fisher, N.; Berry, N.; Stocks, P.A.; Meunier, B.; Williams, D.P.; Bonar-Law, R.; Bray, P.G.; Owen, A.; O'Neill, P.M.; et al. Acridinediones: Selective and potent inhibitors of the malaria parasite mitochondrial bc(1) complex. *Mol. Pharmacol.* **2008**, *73*, 1347–1355. [[CrossRef](#)]
106. Capper, M.J.; O'Neill, P.M.; Fisher, N.; Strange, R.W.; Moss, D.; Ward, S.A.; Berry, N.G.; Lawrenson, A.S.; Hasnain, S.S.; Biagini, G.A.; et al. Antimalarial 4(1H)-pyridones bind to the Qi site of cytochrome bc1. *Proc. Natl. Acad. Sci. USA* **2015**, *112*, 755–760. [[CrossRef](#)]
107. Biasini, M.; Bienert, S.; Waterhouse, A.; Arnold, K.; Studer, G.; Schmidt, T.; Kiefer, F.; Gallo Cassarino, T.; Bertoni, M.; Bordoli, L.; et al. SWISS-MODEL: Modelling protein tertiary and quaternary structure using evolutionary information. *Nucleic Acids Res.* **2014**, *42*, 252–258. [[CrossRef](#)] [[PubMed](#)]